FACTORS INFLUENCING PERMEABILITY AND DIFFUSION OF RADON IN SYNTHETIC SANDSTONES

By

Hilton B. Evans

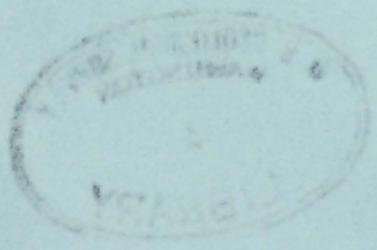

FACTORS INFLUENCING PERMEABILITY AND DIFFUSION OF RADON IN SYNTHETIC SANDSTONES

by

Hilton B. Evans

U. S. Geological Survey
OPEN FILE REPORT

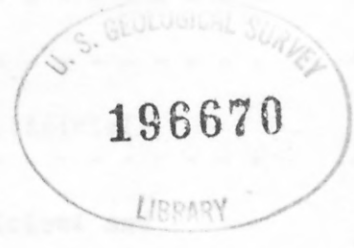

TABLE OF CONTENTS

LIST OF ILLUSTRATIONS

Figure page

LIST OF TABLES

ACKNOWLEDGMENTS

The writer expresses appreciation to Professor K. L. Cook for his suggestions and assistance in preparing this thesis. Professor J. W. Berg, Jr. read the thesis and offered helpful suggestions. Professor F. W. Christiansen has also read the thesis and offered comments. A. H. Lauchenbruch of the U. S. Geologic Survey and J. H. Wolfe of the Mathematics Department of the University of Utah contributed valuable suggestions concerning the mathematics of the diffusion process. A. B. Tanner of the U. S. Geological Survey suggested the possibility of determining nonequilibrium radon concentrations by the method developed in the thesis.

The ~~Geophysics Branch of the~~ U. S. Geological Survey and the Research Division of the Atomic Energy Commission provided the equipment and the financial support necessary to complete the investigation.

The cores were made in the geophysics laboratory of the University of Utah.

ABSTRACT

Artificial sandstone cores were constructed in which the porosity, cement content, and grain size were controlled. Except for the two ends, the cores were sealed in lucite.

The relation between the permeability k (millidarcys) and the fractional porosity Φ of artificial cores, in which only the porosity varied, was found to be of the form $k=\alpha e^{\beta\Phi}$ (where α and β are factors dependent on the grain size and cement content). The relation between the permeability k (millidarcys) and the mean grain size g (cm) of cores in which only the grain size varied was found to be of the form $k=\gamma g^{\sigma}$ (where σ and γ are factors dependent on the porosity and cement content).

A diffusion system, consisting of two ionization chambers connected by a section of tygon tubing containing an artificial core, was developed to measure the apparent diffusion coefficient of radon in an argon-saturated core. Emperical methods were developed to correct the observed diffusion coefficients for the effect of the length of the tubing connecting the two chambers and for the effect of nonequilibrium between radon and the decay products in the chambers.

The apparent diffusion coefficients of cores, in which the porosity and grain size were constant, were found to increase with decreasing cement content. For cores in which only the porosity varied, the apparent diffusion coefficients increased with increasing porosity. No clear relationship could be established between the apparent diffusion coefficient and the mean grain size of cores in which only the grain size varied although the general trend indicated that the apparent diffusion coefficient increased with increasing grain size.

INTRODUCTION

Diffusion in porous media

The migration of a substance under the action of a difference in chemical potential (in response to a concentration gradient or partial pressure gradient) is called diffusion. When a steady state condition exists, the quantity of diffusing material crossing a unit area per unit time is proportional to the gradient of concentration. The proportionality factor is called the diffusion coefficient and is normally expressed in cm^2/sec. Thus, the diffusion coefficient is analogous to the specific electrical conductance. Diffusion of a solute in water or of a gas in air is called free diffusion, and the diffusion coefficient obtained under these conditions is normally referred to as the true diffusion coefficient.

When diffusion takes place in the water or air contained in the pore space of a porous medium, the rate of transfer of material is reduced by the tortuous diffusion path through the pores. In this case the observed diffusion coefficient is referred to as the apparent diffusion coefficient.

The diffusion of a gas through a porous medium is influenced by the presence of moisture, by the molecular weight of the diffusing substance, and, in extreme cases, by the size of the pore spaces through which the gas diffuses. Regardless of the medium through which a gas diffuses, the observed diffusion coefficient is dependent on the temperature and pressure conditions existing when diffusion occurs (Schwertz and Brow, 1951).

Because of its relatively long half-life (3.825 days), the radioactive gas radon (Ra^{222}), generated by a source of parent material (Ra^{226}) in the ground, can migrate through several meters of porous rock and soil under favorable conditions. The quantity of radon diffusing through a layer of rock or soil is dependent on the moisture content and physical properties of the layer through which diffusion occurs and on existing meteorological conditions.

The ability of radon to migrate allows it to be used in tracing geologic features and detecting radioactive ore deposits by soil gas sampling methods. The results of these soil gas surveys can be more easily interpreted when the influence of rock and soil structure on the migration of radon by diffusion is known.

Purpose and scope of present investigation

Although it is known that radon migrates through porous rock, little is known of the relative importance of diffusion phenomenon in the process. It is the purpose of the present study to attempt to establish some of the properties of the diffusion process by experimental techniques so that its importance can be better understood and evaluated quantitatively.

Laboratory and field determinations of the diffusion coefficient of various gases in soils and other porous materials have been carried out not only to aid in understanding the factors influencing gaseous diffusion in porous media, but to investigate the possibility of measuring radioactive gas in soil air for the purpose of locating deposits of radioactive materials. Because of the difficulty in isolating the effect of individual factors such as porosity, cement content, and grain size, the influence of each of these factors on the diffusion of radioactive gases through consolidated rocks has been only partially investigated.

The investigation reported here constitutes an attempt to determine experimentally the effect of porosity, cement content, and grain size on the diffusion of radon through consolidated argon-filled porous media. In order to evaluate the effect of these factors individually, artificial sandstone cores were constructed in which the porosity, cement content, and grain size were controlled. The permeability and porosity of these cores were determined, and measurements of the apparent diffusion coefficient of radon in about 20 of the cores were carried out. The results were then related, as far as possible, by plots of the data obtained.

The purpose of this investigation was not to obtain absolute measurements of either diffusion coefficients or permeability, but to show the variation of apparent diffusion coefficient and permeability with core characteristics.

Previous investigations

Since the early investigations concerned with determining the quantity of radon in soil air (Bumstead and Wheeler, 1904; Satterly, 1912), a number of researchers have attempted to relate diffusion of the radioactive gases, radon and thoron, through porous media to such factors as porosity, moisture content, and particle size.

The laboratory apparatus commonly employed to determine the coefficient of diffusion of radioactive gases through soils or rocks consists of a closed system containing a gas source and an ionization chamber (with attached electrometer) separated by a layer of soil or rock. The measured change in concentration on one or both sides of the layer of material can be related to the diffusion coefficient by obtaining, with the appropriate boundary conditions, a solution of the diffusion equation. The diffusion equation, which is designated Fick's Second Law of Diffusion, for a substance decaying by radioactive emission is

$$\frac{\partial C}{\partial t} = D\nabla C - \lambda C$$

where C is the concentration of the diffusion material in curies/liter, λ is the decay constant in sec^{-1},

$$\nabla = \frac{\partial}{\partial x} + \frac{\partial}{\partial y} + \frac{\partial}{\partial z}$$

D is the diffusion coefficient (independent of concentration) in cm^2/sec and $\partial C/\partial t$ is the rate of change of concentration (curies/liter/sec).

Using the apparatus and method described above, Grammakov (1936) determined the effect of moisture content on the diffusion of Thoron

(Ra^{220}, half-life 52 sec) in the air (with moisture present) of layers of quartz sand and loam. The porosity of both types of sand was about 40 percent when dry. The reduction in diffusion coefficient with increasing moisture content of the sand is illustrated in figure 1 for both types of sand. The effect of the two types of sand in reducing the diffusion coefficient was essentially the same for a particular moisture content.

The diffusion coefficient was determined by relating the flux of radioactive gas into the ionization chamber to the flux of radioactive gas from the source material as follows:

$$Q = Q_e \operatorname{csh} h\sqrt{\lambda/D_a} \qquad (1)$$

where

Q = flux from the source layer (curies/cm^2 sec).

Q_e = flux into the ionization chamber (curies/cm^2 sec).

h = thickness of the sand layer (cm).

λ = decay constant of thoron = 1.33 X 10^{-2} sec^{-1}.

D_a apparent diffusion coefficient in the sand layer (cm^2/sec).

Using essentially the same apparatus and technique, Gracheva (1938) measured the diffusion coefficient of thoron diffusing through layers of quartz sand. The individual layers were composed of quartz grains representing a narrow range of grain diameters (0.2 mm to 5.0 mm), and the porosity of each layer was between 42 percent and 45 percent. Gracheva concluded that the diffusion coefficient was independent of the grain diameter in the range 0.2 mm to 5.0 mm. Figure 2 shows a plot of percentage ratio of the emanation flux through a layer of thickness h to the flux through a layer one cm thick (for four grain sizes)

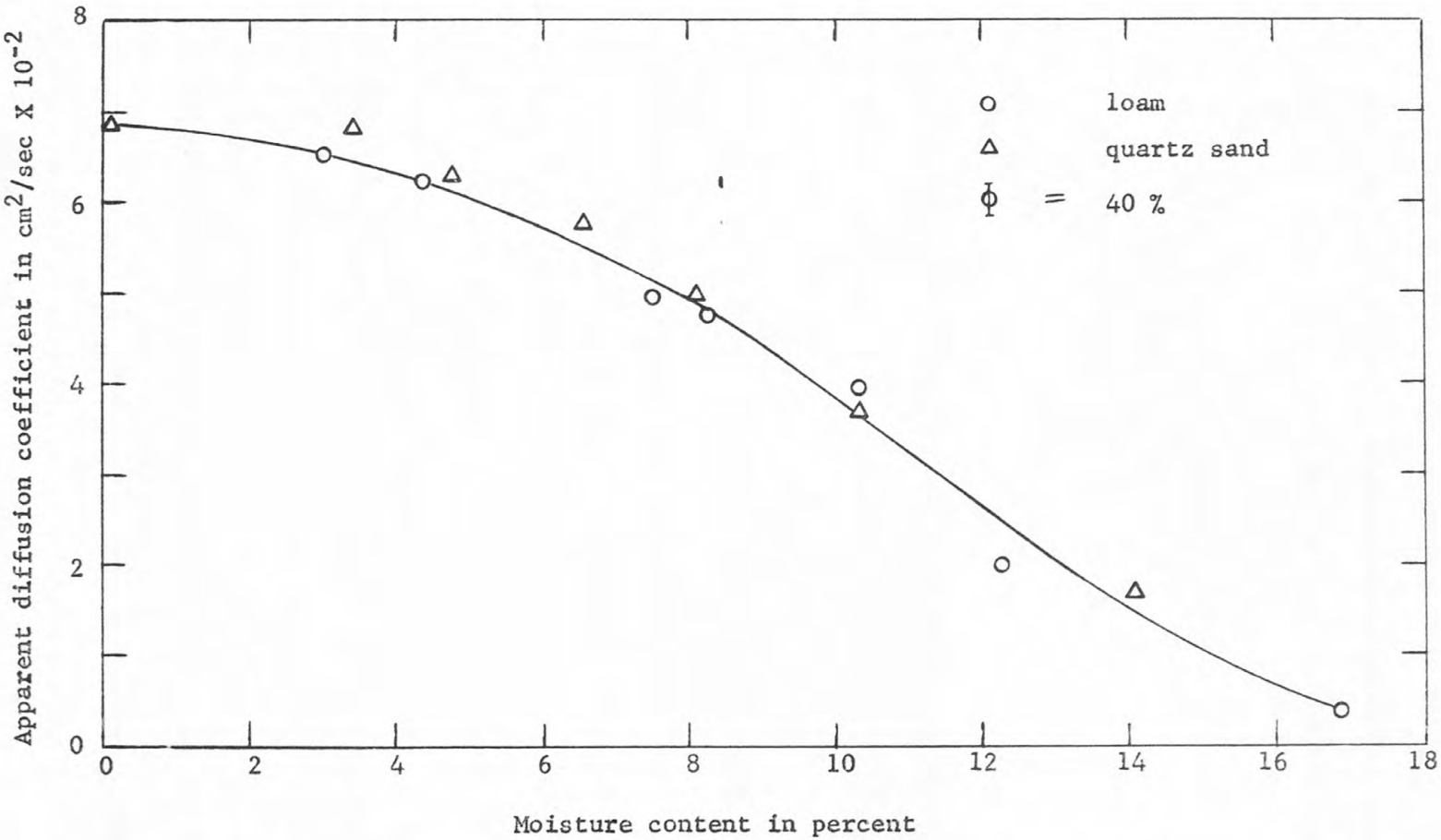

FIGURE 1.- Dependence of apparent diffusion coefficient of thoron on moisture content of loam and quartz sand (after Grammakov, 1936).

for layers of various thicknesses. Figure 2 also shows the theoretical curve for this percentage ratio, as obtained by Gracheva, assuming a steady state and taking D_a as 0.045 cm^2/sec; the curve was plotted from the equation

$$\frac{Ie}{Ie_1} = \frac{csh\ h\sqrt{\lambda/Da}}{csh\ h\sqrt{\lambda/Da}} \qquad (2)$$

where

I_e = flux (curies/cm^2) at a distance h (cm) from the source.

Ie_1 = flux through a layer one cm thick (curies/cm^2).

λ = decay constant of the emanation = $1.33 \times 10^{-2}/sec^{-1}$.

and

D_a = the apparent diffusion coefficient in the layer (cm^2/sec).

In order to determine the effect of porosity on the diffusion of radioactive gas, Gracheva measured the diffusion of thoron through plates of unglazed porcelain having porosities of 12.5 percent, 7.4 percent, and 6.2 percent; the apparent diffusion coefficients obtained were 0.005 cm^2/sec, 0.0027 cm^2/sec, and 0.002 cm^2/sec, respectively. On the basis of these measurements and of earlier investigations concerning the diffusion of CO_2 through soils (Buckingham, 1904), the diffusion coefficient was found to be proportional to the square of the porosity.

In contrast to the results of Gracheva, experiments by Penman (1940) using CS_2 diffusing through artifically packed columns of soil indicate that the diffusion coefficient is proportional to the porosity. In addition, measurements of the diffusion coefficient of radon in columns

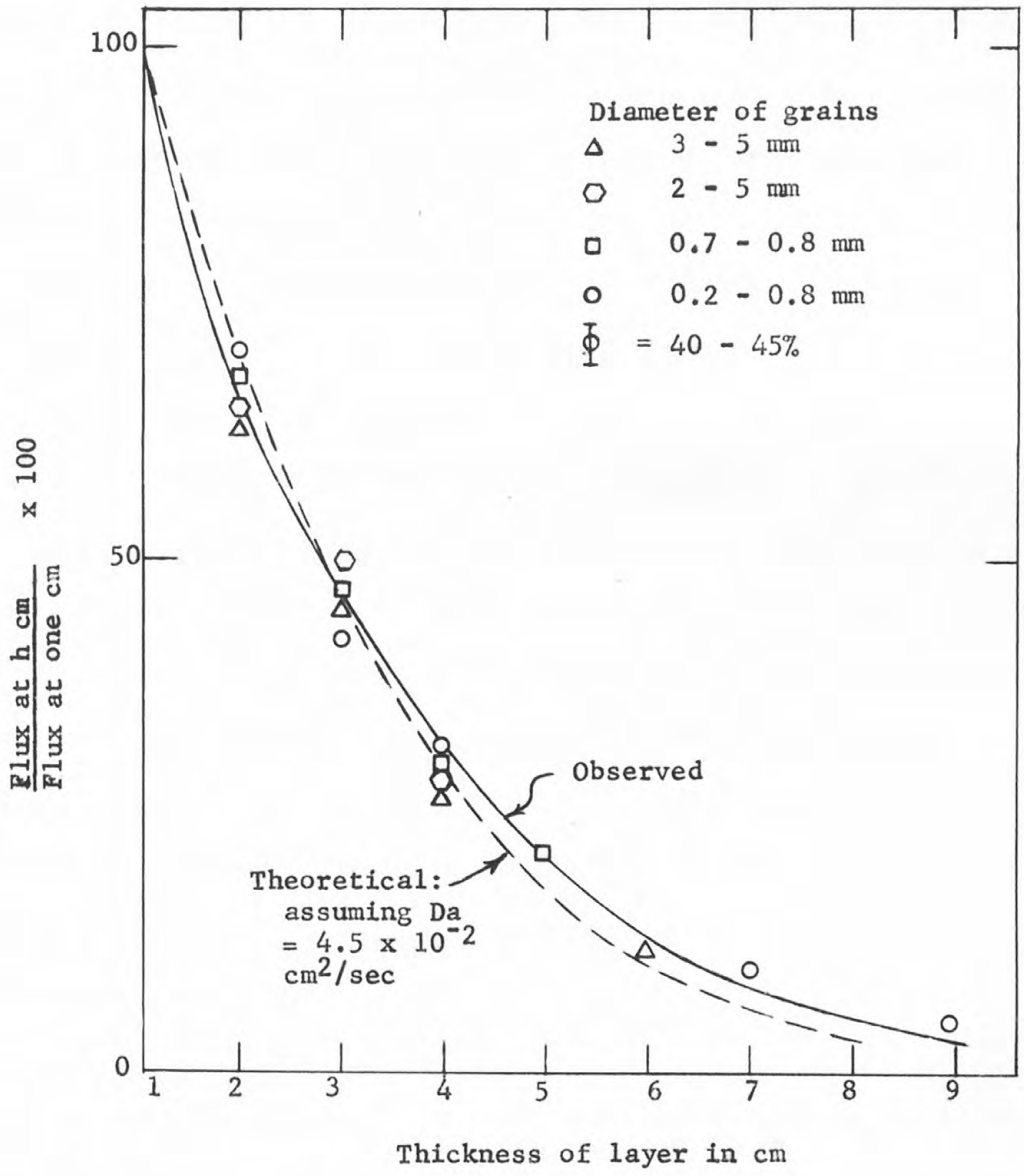

FIGURE 2.- Effect of layer thickness on the thoron flux through layers of quartz sand each containing a different mean grain size (after Baranov and Gracheva, 1937).

of moist sands (Budde, 1958) indicate that the diffusion coefficient decreases as the predominate grain size decreases. According to Budde the diffusion coefficient was less than 10^{-5} cm^2/sec for a grain size of 0.02 mm and 12×10^{-3} cm^2/sec for a grain size of about 0.3 mm. The diffusion coefficient found by Budde for the different soils in a dry state was approximately that of radon in air, namely about 10^{-1} cm^2/sec.

Garrels and others (1945) measured the diffusion of potassium permanganate and KCl solutions through limestone cores 1 to 2 mm thick and 2 cm in diameter, which were saturated with water. They found that the amount of material moving through the rock was independent of the pore size except for pores approaching the diameter of ions. They concluded from these measurements that the rate of penetration of the ionic materials through intergranular openings in water-saturated rocks is independent of the porosity or permeability of the rock but dependent on a parameter designated by them as the "effective directional porosity". The effective directional porosity was defined by them as the product of the ratio of the effective area of a core to the effective length and the ratio of the true length to the true area, or

$$A'L/AL'$$

where the primes denote the effective values. In general, the effective area and length of a core differed from the true area and length. The value of A'/L' is obtained from the equation for steady state diffusion assuming the diffusion coefficient to be that of the material diffusing in water. This equation is given by

$$\frac{A'}{L'} = \frac{V}{D_o t} \ln \frac{\Delta C_o}{\Delta C_t}$$

where

V is the volume of the compartment containing solution on either side of the core (cm^3),

t is the time of diffusion (sec),

ΔC_o is the difference in concentration (equivalents/liter) of the diffusing substance between the compartments at the beginning of the run,

ΔC_t is the difference in concentration (equivalents/liter) between the two compartments at time t, and

D_o is the true diffusion coefficient (cm^2/sec) of the material diffusing in water.

The ratio of the measured porosity Φ to the effective directional porosity is designated by Garrels and others (1945) as the "lithologic factor" and is convenient in describing the influence of rock structure on the transport of materials through the rock by diffusion. For unconsolidated sands, the lithologic factor varies between 1.4 and 2.0. For consolidated sandstones, the lithologic factor is increased by the presence of cementing material and may vary from 2 to 5 or higher.

Klinkenberg (1951) confirmed the work of Garrels and others (1945) and showed that the effective directional porosity and the lithologic factor of rocks is the same for either electrical conduction or diffusion and can be easily obtained by measuring the electrical conductivity of a rock saturated with a solution of known conductivity.

Baranov and Novitskaya (1949) obtained a value of 0.72×10^{-5} cm^2/sec for the diffusion coefficient of radon in organic muds and 1.6×10^{-5} cm^2/sec in mineral muds at the same temperature (46° C). Since the moisture

content of the two muds was essentially the same, the smaller diffusion coefficient in the organic mud could result either from adsorption of the radon on the organic matter or from a reduction of continuous pore space available to the diffusing radioactive gas.

Reports of investigations concerning the diffusion of radioactive gas in rocks and the influence of rock characteristics on the quantity of radioactive gas transferred by diffusion could not be found in the literature. A brief list of the diffusion coefficients of radioactive gases obtained under various conditions is presented in table 1.

Table 1

Diffusion coefficients of radioactive gases

in various media

Source	Radioactive gas	Medium of diffusion	Measured diffusion coefficient cm^2/sec
Baranov and Novitskaya 1949	radon	quartz sand, dry	6.75×10^{-2}
	thoron	quartz sand, dry	6.75×10^{-2}
	thoron	quartz sand, 10.4% moisture	3.75×10^{-2}
	thoron	quartz sand, 15.2% moisture	1.00×10^{-2}
	thoron	powdered clay, air dry	5.00×10^{-2}
	radon	water, 18° C	1.15×10^{-5} *
	radon	air	0.1 *
Aliverti and Lovera 1949	radon	air	0.1 *
		soil	0.013
Hirst and Harrison 1938 and 1939	radon	argon at 760mm and 15° C	0.092 *
		air at 760mm and 15° C	0.120 *
Israel and Becker 1935	radon	soil air	0.05
Mortari, 1933	radon	air	0.11 *
Eckmann, 1913	radon	air	0.07 *
Chaumont, 1910	radon	air	0.1014 *
	radon	air	0.1017 *

* True diffusion coefficients.

Table 1 (continued)

Diffusion coefficients of radioactive gases

in various media

Source	Radioactive gas	Medium of diffusion	Measured diffusion coefficient cm^2/sec
Leslie, 1912	thoron	air	0,085 *
	actinon	air	0,098 *
Bagnall, 1957	radon	water	$7,6 \times 10^{-5}$ *

* True diffusion coefficients.

EXPERIMENTAL PROCEDURE

Construction of artificial cores

The process of constructing artificial cores simulating natural porous sandstone was essentially that employed by Mandel and others (1957) and by Murphy and others (1957). Most of the cores were composed of Ottawa sand grains cemented with commercial Grefco cement or a Grefco-clay (kaolin) mixture; but in order to increase particle size, a few cores were composed of plastic beads. Sand was screened to the desired particle size, mixed with the cementing material in various amounts by percentage by weight, and wetted with 0.1 ml to 0.5 ml of water. The wet cement-sand mixture was then thoroughly stirred, placed in a 3/4-inch diameter steel core barrel, and compressed at pressures ranging from about 300 psi to about 50,000 psi. After pressing, the cores were alternated between a warm humid atmosphere and a drying oven until the cement had completely reacted and the cores had reached a constant dry weight. The cores were then flooded in an evacuated jar and weighed wet. The ratio of the difference between wet and dry weight and the total computed core volume was considered to be the effective porosity. Figure 3 shows the effect of construction pressure on porosity for cores of the same mean grain size (0.043 cm) with cement contents of 25 percent and 40 percent, respectively.

The permeability of about 150 cores was determined although it was necessary to construct approximately 230 cores to obtain the desired core characteristics.

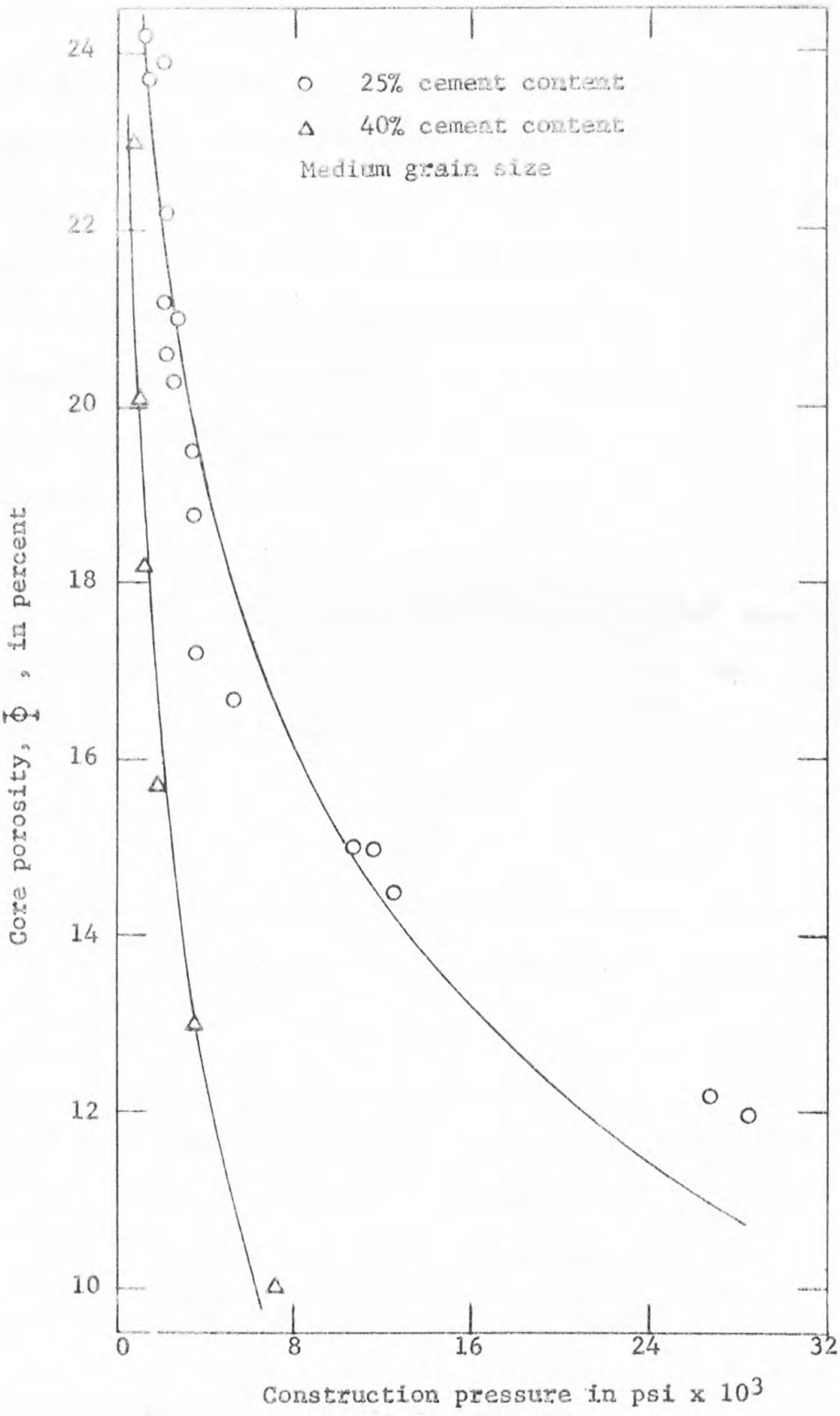

FIGURE 3.- Construction pressure required to produce a particular core porosity for artificial cores containing 25 percent cement and 40 percent cement.

Several sets of cores were constructed which include a suite of cores having a range of porosities (with grain size constant) for six different cement contents, a suite of cores (grain size and porosity constant) for six different cement contents, a suite of cores (cement content and porosity constant) for four different grain sizes, and one suite of cores (cement content and grain size constant but having a range of porosities) in which half of the cementing material was kaolin.

Four average grain sizes were used in core construction which are designated as small, medium, large, and beads. Each grain size consists of the average grain diameter obtained by screening between certain limits. The relation between the grain size reported here and their particle range is listed in table 2.*

Table 2

Mean particle diameter and corresponding particle range

Grain Size	Particle range (cm)	Particle type	Approximate mean particle diameter for a particle range (cm)
Small	0.010 - 0.025	Ottawa sand	0.019
Medium	0.025 - 0.059	Ottawa sand	0.043
Large	0.059 - 0.084	Ottawa sand	0.069
Beads	0.084 - 0.141	Plastic beads	0.107

* All tables following table 2 appear in appendix II.

Sealing artificial cores

It was necessary to seal the cores for laboratory use to eliminate gas loss to the atmosphere. A number of methods of sealing cores were tried, but the most satisfactory method was that of mounting the cores in lucite. The cores were placed, along with powdered lucite, in a steel heating jacket, containing a movable steel cylinder in one end to provide pressure on the lucite during the heating process.. The lucite was heated to 150° C and pressed at about 4000 psi to drive out any water vapor and to solidify the lucite.

After cooling, the ends of the cores were cut off and smoothed to insure free gas passage during permeability determinations. The average diameter of the final cores was about 3/4 inch and the final length was between 1/4 inch and 1 inch.

Permeability determinations

Core permeabilities were determined by a method outlined by Wyckoff and others (1934). The technique requires measurements of the gas pressures on the inflow and outflow side of the core, the barometric pressure, the gas volume flowing through the core per unit time, and the core dimensions. If $\bar{Q}$ is the flow rate of the gas (cm^3/sec) at the average pressure (atm) between the ends of the core, P_1 and P_2 are the pressures (atm) at the ends of the core, and A and L are the area (cm^2) and length (cm) of the core, then

$$k/\eta = \frac{\bar{Q}/A}{(P_1 - P_2)/L} = \frac{\text{Permeability}}{\text{Viscosity}}$$

or

$$k = \eta \frac{\bar{Q}/A}{(P_1 - P_2)/L} = \text{Permeability in darcys}$$

A plot of $\bar{Q}$ versus $(P_1 - P_2)/L$ for each flow rate results in a straight line (for viscous flow). The slope of this straight line is k/η and from k/η the permeability can be found for any gas. Figure 4 is a typical example of a plot of the values of $\bar{Q}$ versus $(P_1 - P_2)/L$ measured for a particular core to obtain the permeability.

In practice, the lucite sealed core was clamped in a short piece of tygon tubing and connected between two mercury manometers. Argon gas under pressure was then forced through one end of the core. The flow time was measured with a stop watch, and the flow volume determined by water displacement in a calibrated vessel. Flow rates at various pressures were measured for each core so that k/η could be determined. The permeability of each core was obtained by multiplying the k/η ratio by the viscosity of argon (221.7 micropoise at 20° C).

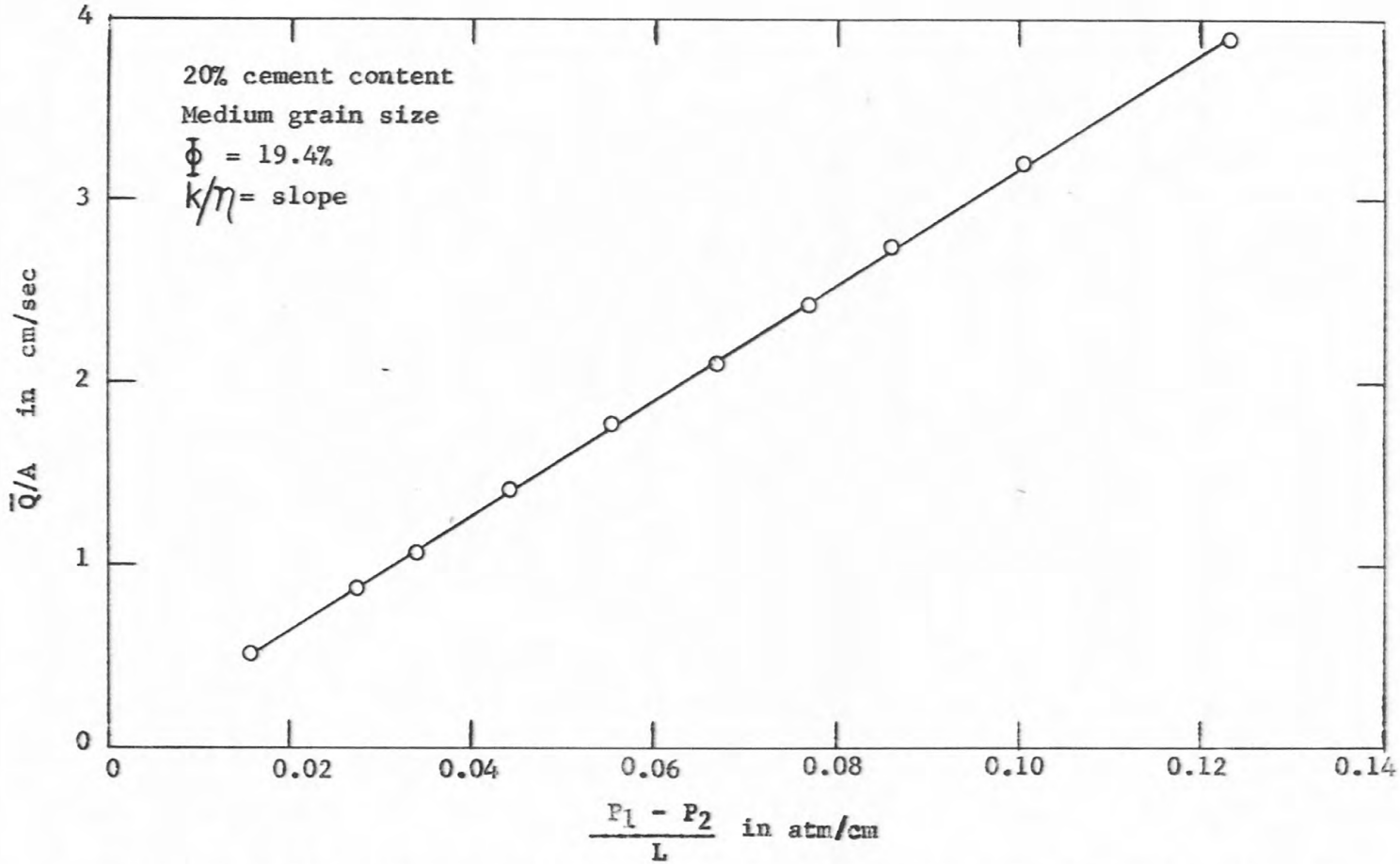

FIGURE 4.- Flow rate per unit area of core versus pressure gradient through core for an artificial sandstone core of 20 percent cement, 19.4 percent porosity, and medium grain.

Diffusion coefficient determinations

Method of measuring radon

Radon is a radioactive gas that is a disintegration product of radium, and by virtue of its relatively long half-life (3.825 days), is especially useful in investigations where a gaseous tracer is required. Since radon emits alpha particles in disintegrating, it can readily be detected by measuring the ionization produced by the alpha particles moving through a gas such as argon, for example. In order to observe the effects of ionization, a voltage is applied to the ionization chamber. The applied electric field sweeps out the ion products so that a current is produced that is proportional to the alpha activity. The ion current produced in the argon-filled ionization chamber is amplified in a vibrating reed electrometer and the integrated current recorded on a strip-chart recorder. In the present work an Applied Physics electrometer and a continuously recording strip-chart Esterline Angus recorder were used to measure and record the current produced by the disintegration of radon in the ionization chamber.

Because the amount of radioactivity in the ionization chamber was recorded in terms of current or voltage, it was necessary to calibrate the chambers in terms of the ion current produced by a known amount of radon in equilibrium with its decay products. Radon concentrations are generally expressed in micro-micro curies/liter ($\mu\mu C/l$) where a curie is defined as the amount of radon in equilibrium with a gram of radium and is equivalent to 3.7×10^{10} disintegrations per second. Calibration coefficients, determined for each chamber and electrometer, are expressed in $\mu\mu C$ per millivolt so that recorder readings can be readily converted to $\mu\mu C$.

The "background" consists of the residual current present in an argon-filled ionization chamber due to radioactive impurities in the chamber material, cosmic rays, electronic noise, and other sources of current not associated with the radioactive decay of a sample in the ion chamber. The background must be subtracted from any sample determination before calibration and decay corrections are applied.

Standard radium chloride solutions obtained from the National Bureau of Standards served as the source of radon. These radium solutions (10^3 and 10^5 $\mu\mu C$ samples) were stored in reflux condensers and boiled periodically to obtain the radon produced by the radium disintegration. The radium solutions were boiled for approximately 20 minutes to insure complete de-emanation of the sample and, during the de-emanation period, argon was bubbled through the solution to aid in transporting the radon into the ionization chamber. The gas handling system is essentially the same as the system described by Rogers (1958).

Diffusion system

In order to determine the diffusion coefficient of radon moving through an argon-saturated porous core, an experimental system similar to that previously described by Baranov and Gracheva (1937) and Budde (1958) was used. However, an ionization chamber containing radon was used in place of a source layer or solution. A sketch of the essential features of the diffusion system is shown in figure 5.

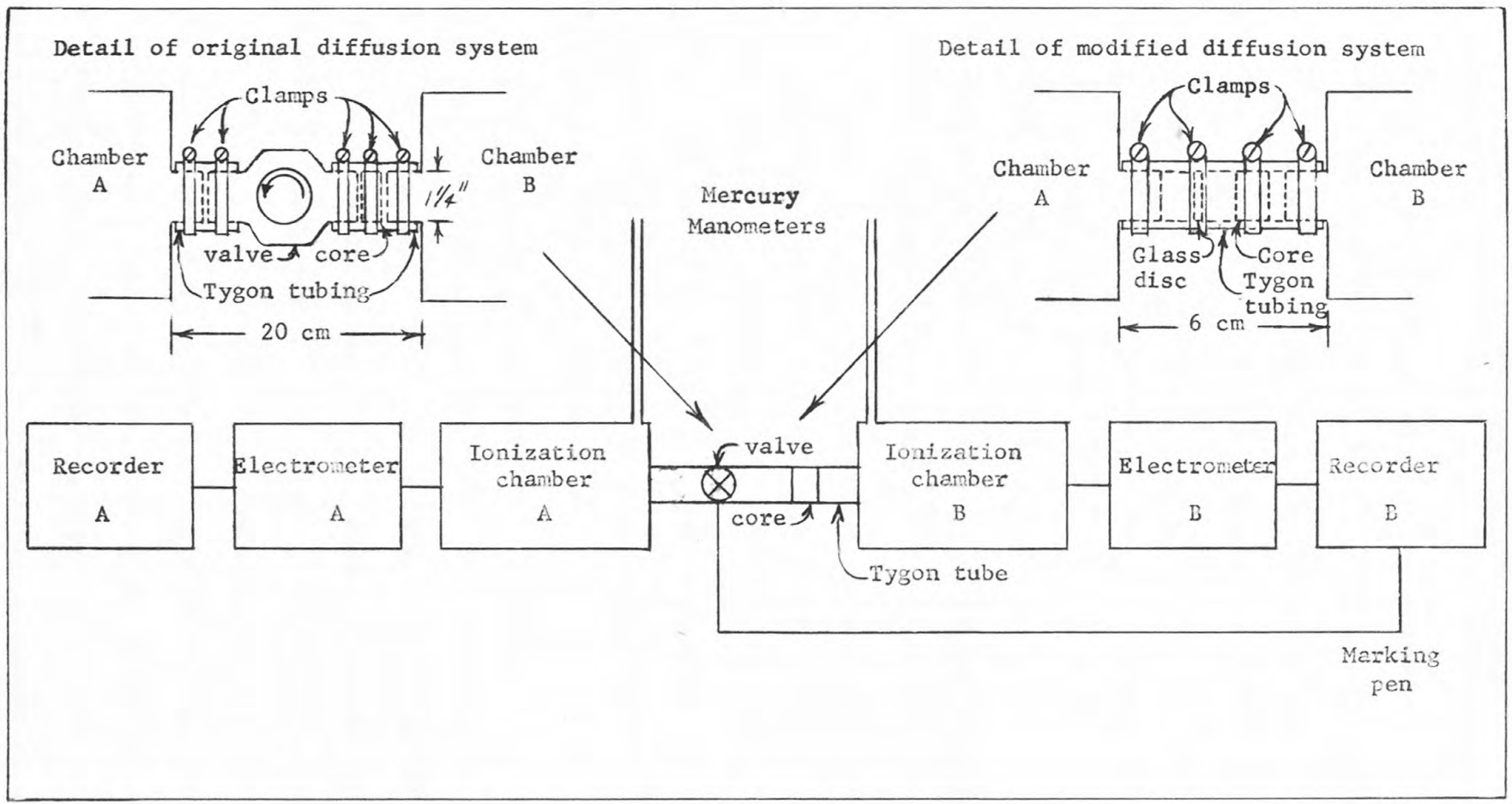

FIGURE 5.- Sketch of instrumentation used in determining diffusion coefficients, showing original diffusion system and modified diffusion system.

Original diffusion system

Fore the earlier measurements, a ball-type valve (Chemtrol Co.) with an effective open diameter of 1 1/4 inches was attached to chamber A (fig. 5) with tygon tubing of 1 1/4-inch inside diameter. A lucite-sealed core was placed in a section of tygon about 2 inches long and clamped in place so that no diffusion could occur between the lucite cylinder and the tubing wall. One end of the tygon tubing containing the core was then attached to the valve and the other end was attached to chamber B. With the valve in place, the two chambers were isolated and either chamber could be evacuated or filled independently. After all connections were made, the separation between the chambers was about 8 inches.

The experimental procedure was as follows: First, each of the ionization chambers was flushed with dry argon to remove any radon and suspended decay products remaining in the chambers. After flushing, it was necessary to allow the radon decay products attached to the chamber walls to decay until the background in each chamber reached a steady value. Both chambers were then evacuated and the valve was closed to isolate the two chambers. With the valve closed, chamber B (the receiving chamber) was then filled separately with argon; and radon was next boiled into chamber A separately from a radium chloride solution (10^{-7} gm of radium in 200 ml of distilled water) using argon to transport the radon into chamber A. Both chambers were filled to atmospheric pressure. It was then necessary to wait about four hours to allow the radon in chamber A to reach equilibrium with its daughter products, and at this time, the concentration of radon was ordinarily about 70,000 $\mu\mu$C to 90,000 $\mu\mu$C.

At the end of the four-hour period the valve was opened, and the radon was allowed to diffuse from chamber A through the core into chamber

B for a period of 12 hours to 20 hours in most of the measurements. As the radon diffused through the core, the radon concentrations in the two chambers was continuously charted as a function of time by the corresponding recorders. The chart speed was about three inches per hour.

Since the volume of radon in either chamber (a maximum of about 8×10^{-8} cc) was always negligible compared with the volume of the argon in either chamber (4×10^{3} cc), the concentration of argon in each chamber remained constant, and, during the diffusion run, both chambers remained at atmospheric pressure.

In a few of the measurements, the valve was turned off after diffusion had taken place for four hours, and the system was again allowed to reach equilibrium. These equilibrium concentrations in the two chambers were then compared with the recorded concentrations (nonequilibrium) in order to determine the degree of nonequilibrium existing at the end of the first four hours of a 12-hour to 20-hour run.

To terminate the diffusion run, the valve was closed, a new core was clamped in the tygon tube, and the connection between the valve and chamber B was reestablished. Normally, a sufficient concentration of radon remained in chamber A so that 6 to 8 separate runs could be carried out, in an equivalent number of days, before it was necessary to reboil the radium chloride solution to refill chamber A.

In order to minimize the error in measuring the radon concentration, no runs were conducted when the radon concentration in chamber A was less than about 10,000 $\mu\mu$C. In chamber B, the radon concentration did not exceed 5,000 $\mu\mu$C (at the end of four hours) when the radon concentration in chamber A was a maximum. When the radon concentration in chamber A had decreased to about 10,000 $\mu\mu$C, the radon concentration in chamber B normally would not exceed a few hundred $\mu\mu$C after four hours.

Modified diffusion system

For the later measurements, the separation between the ionization chambers was reduced to about 6 cm. In this series of runs, the valve was replaced by a thin glass disc about 34 mm in diameter. The glass disc was inserted into the tygon tubing between the core and chamber A and clamped in place to isolate the two chambers. Using the modified system, the procedure for runs was the same as that described for the original system except that the glass disc was crushed to allow the radon to diffuse from chamber A through the core to chamber B. This technique was used to eliminate the diffusion time associated with the valve and connecting tubing so that the effect of the tubing (now only about 6 cm long) on the diffusion coefficient was minimized.

Evaluation of diffusion measurements

Theoretical development

Considering the system shown in figure 5, let V_1 and V_2 be the volumes (cm^3) of ionization chambers A and B, respectively; c_1 and c_2 be the radon concentrations ($\mu\mu C$) in the chambers A and B, respectively, at time t (sec), let L and A be the length (cm) and area (cm^2) of the porous core between the two chambers, let D_a be the apparent diffusion coefficient (cm^2/sec) of radon moving through the core and λ be the decay constant of radon (sec^{-1}). Since the change in the amount of radon in the chamber at time t must equal the quantity that has diffused into or out of the chamber, assuming steady state, in chamber A,

$$V dc_1 + (D_a A/L)(c_1 - c_2)dt + V_1 \lambda c_1 dt = 0 \qquad (3a)$$

and in chamber B,

$$V_2 dc_2 - (D_a A/L)(c_1 - c_2)dt + V_2 \lambda c_2 dt = 0 . \qquad (3b)$$

The term containing λ is the decrease in material resulting from radioactive decay. Combining (3a) and (3b) gives:

$$\frac{d(c_1 - c_2)}{(c_1 - c_2)} = -\left[(D_a A/L)(1/V_1 + 1/V_2) + \lambda\right] dt . \qquad (4)$$

Let $\Delta c = c_1 - c_2$ and $A/L\,(1/V_1 + 1/V_2) = b$

then $$\frac{d\Delta c}{\Delta c} = -(D_a b + \lambda)\, dt .$$

If b, which is designated the cell factor, remains constant throughout the diffusion experiment, equation (4) can be integrated as follows:

$$\int_{\Delta c_0}^{\Delta c_t} \frac{d\Delta c}{\Delta c} = \int_0^t -(b D_a + \lambda)\, dt.$$

Where Δc_0 is the initial concentration difference between the two chambers, and Δc_t is the concentration difference at time t, the final equation is:

$$\ln \frac{\Delta c_0}{\Delta c_t} = (b D_a + \lambda) t \,. \qquad (5)$$

Except for the λ term, this is the equation commonly used to evaluate the diffusion coefficient (Gordon, 1945; Andrew, 1955).

If Δc_0 and ($b D_a + \lambda$) are known, the concentration difference at any time t is given by:

$$\Delta c_t = \Delta c_0 e^{-(b D_a + \lambda) t} \,. \qquad (6)$$

When the radon concentrations in the two chambers are corrected for radioactive decay, equations (3a) and (3b) can be reduced to the corresponding equations for a nonradioactive gas by the substitution $c_1 = C_1 e^{-\lambda t}$ and $c_2 = C_2 e^{-\lambda t}$.

Thus, equation (3a) would be

$$V_1 d\frac{(C_1 e^{-\lambda t})}{dt} + (D_a A/L)(C_1 - C_2) e^{-\lambda t} + V_1 \lambda C_1 e^{-\lambda t} = 0.$$

However, $d\frac{(C_1 e^{-\lambda t})}{dt} = \frac{dC_1}{dt} e^{-\lambda t} - \lambda C_1 e^{-\lambda t}$ so that

equation (3a) reduces to:

$$V_1 \frac{dC_1}{dt} + (D_a A/L)(C_1 - C_2) = 0. \qquad (7a)$$

Similarly, equation (3b) can be reduced to:

$$V_2 \frac{dC_2}{dt} - (D_a A/L)(C_1 - C_2) = 0. \qquad (7b)$$

If ΔC_0 is the initial difference in concentration between the two chambers A and B and ΔC_t is the difference in concentration between the same chambers at time t, the integrated equation equivalent to (5) would be

$$\ln \frac{\Delta C_0}{\Delta C_t} = b D_a t \, . \qquad (8)$$

Providing the ratio of the concentration differences $\Delta C_0/\Delta C_t$ and b are known, equation (5) or (8) can be used to evaluate the apparent diffusion coefficient.

When steady state cannot be assumed, it is necessary to obtain a solution of the diffusion equation ($\partial C/\partial t = D\partial^2 C/\partial x^2 - \lambda C$ for diffusion in the x direction) with the appropriate boundary conditions at the ends of the core (see Appendix I).

Some difficulties exist in the use of the diffusion system (fig. 5). The cell factor b (equation (5)) contains the term L/A . This term can be considered to represent the ratio of the effective diffusion length to the effective area through which diffusion occurs. Thus, L/A differs from the ratio of the measured core length to the measured core area by a factor dependent on the tortuosity of the diffusion path in the core and on the length and area of the tygon holding the core and providing a connection between the two chambers.

In view of the fact that the apparent diffusion coefficients obtained using equation (8) appeared to be dependent on the length of the core in cores of similar composition, a relatively homogeneous sandstone core 1.96 cm in length was cut to different lengths (0.91 cm, and 0.36 cm) and

the apparent diffusion coefficient of each section was determined. The permeability and porosity of each section was determined and for sections of core approximately 0.36 cm, 0.91 cm, and 1.96 cm in length the permeabilities and porosities were essentially identical. However, using the measured lengths and areas and equation (8), the apparent diffusion coefficients were larger for the longer cores. The apparent diffusion coefficients for the three lengths of sandstone core are shown in figure 6. Since the permeability and porosity of the three sections was the same in each case, the difference in the apparent diffusion coefficient of these sections was assumed to be related to the diffusion in the connecting tygon tubing and the valve.

In order to determine the effect of diffusion in the connecting tygon tubing and valve on the apparent diffusion coefficient, runs were made using two of the sandstone cores (0.36 cm and 0.91 cm), in a modified version of the diffusion system shown in figure 5. In the modified system the valve was replaced by a thin glass disc designed to shatter under radial pressure, and the ionization chambers were connected with a short (6 cm) length of tygon tubing. Crushing the disc was equivalent to opening the valve to initiate the diffusion process. The use of a glass disc allowed the chamber separation to be reduced to about 20 percent of that necessary when the valve was used (8 inches).

This reduction in chamber separation resulted in about the same apparent diffusion coefficient for the two shorter sections of sandstone core (0.36 cm and 0.91 cm) as that obtained for the longer section (1.96 cm) using the system containing a valve. Since sections of a homogeneous medium should yield the same apparent diffusion coefficient regardless of

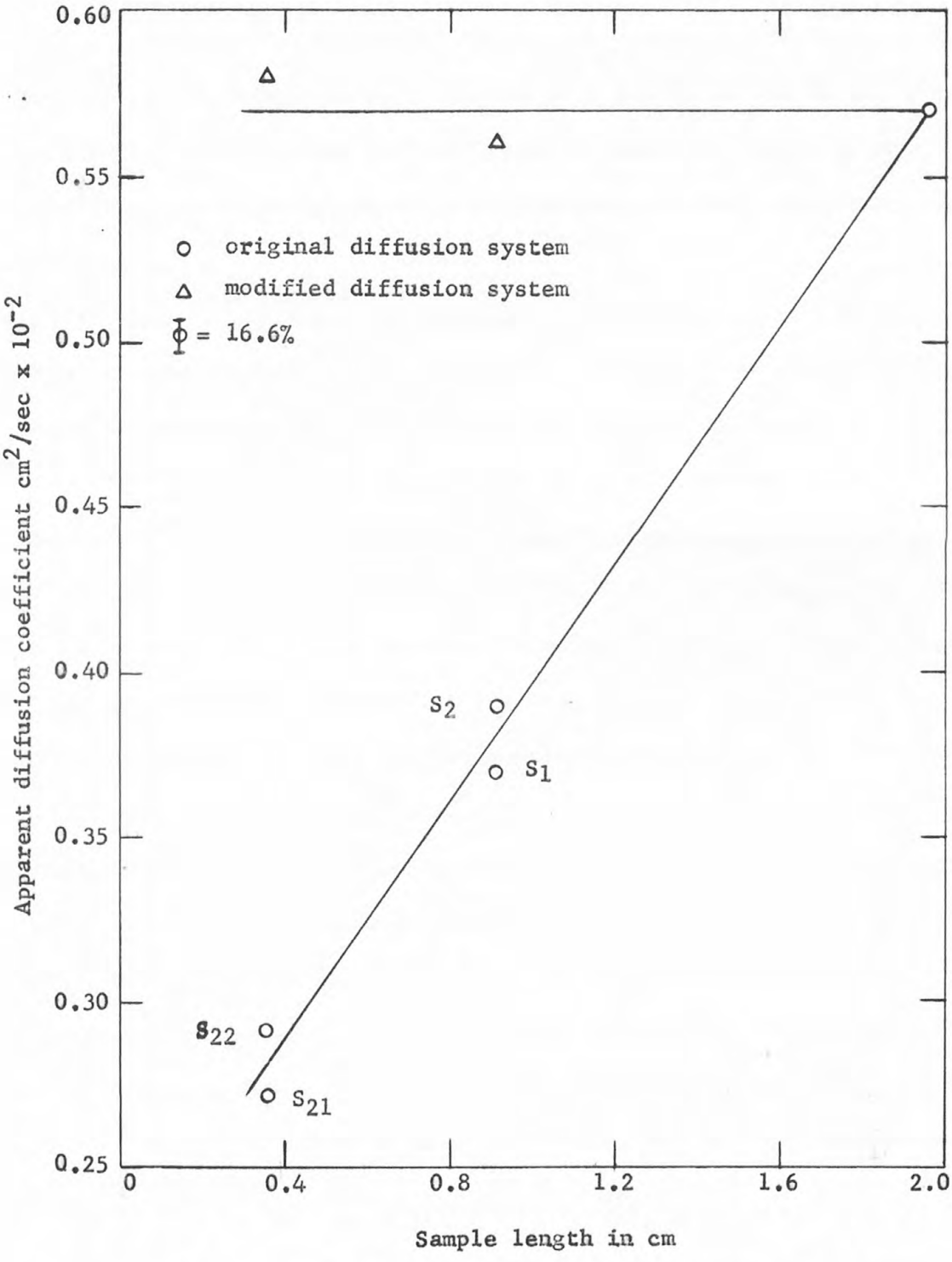

FIGURE 6.- Effect of sample length on apparent diffusion coefficient of radon in sections of a natural, homogeneous sandstone of 16.6 percent porosity.

their length, it was reasonable to assume that the influence of the tygon tubing and valve on apparent diffusion coefficients determined in the system of figure 5 was negligible providing the cores were approximately 2 cm in length.

Correction of the observed apparent diffusion coefficient for the effect of the tubing was necessary for three series of artificial cores. The correction was obtained by measuring the apparent diffusion coefficient of four cores representative of the range of lengths in each series using the modified diffusion system. The apparent diffusion coefficients for cores measured in the modified diffusion system were then plotted as a function of the core length and a straight line (least mean square curve) was drawn through the data points. The apparent diffusion coefficients of the remaining cores in the series were adjusted to this curve. The magnitude of the correction was proportional to the length of the core, and as a result of the correction for the longer tygon tubing the apparent diffusion coefficient of each core was increased.

Because preparation for a diffusion run required approximately twice as long as in the system containing a valve, and because shattering the glass disc was a difficult and uncertain process, this system was used in only a few runs to provide a means of correcting the apparent diffusion coefficients for the effect of the tubing and valve.

Equilibrium considerations

A second difficulty arises in the use of a flow system when the quantity of radon is to be measured in an ionization chamber calibrated in terms of a quantity of radon in equilibrium with its decay products. When a quantity of pure radon is introduced into a chamber, the radon does not reach equilibrium with its decay products for approximately four hours. The fraction of the equilibrium activity as a function of time is shown in figure 7 for radon and the two short-lived decay products RaA (P_o^{218}) and RaC' (P_o^{214}). RaA and RaC', like radon, are alpha emitters and are the only short-lived radon daughters of interest in ionization chamber measurements. In the diffusion system, radon flows into the chamber continuously so that complete radioactive equilibrium requires three to four times the normal four-hour period.

Experimentally, the equilibrium concentrations in the two chambers at any time during the diffusion process can be determined by closing the valve and waiting four hours for the mixture of radon and daughters to reach equilibrium. Frequently, this method was employed to determine radon concentrations.

It was often desirable to allow the diffusion process to continue for a period of several hours or days in order to obtain a continuous record of the change in radon concentration in the two chambers (figure 8). In this case, equilibrium concentrations could not be measured during the early part of the run and it was necessary to correct the recorded concentrations, either empirically or mathematically, to the equilibrium values existing at any particular time during the diffusion process. Non-equilibrium in chamber B resulted in recorded concentrations 10 to 30

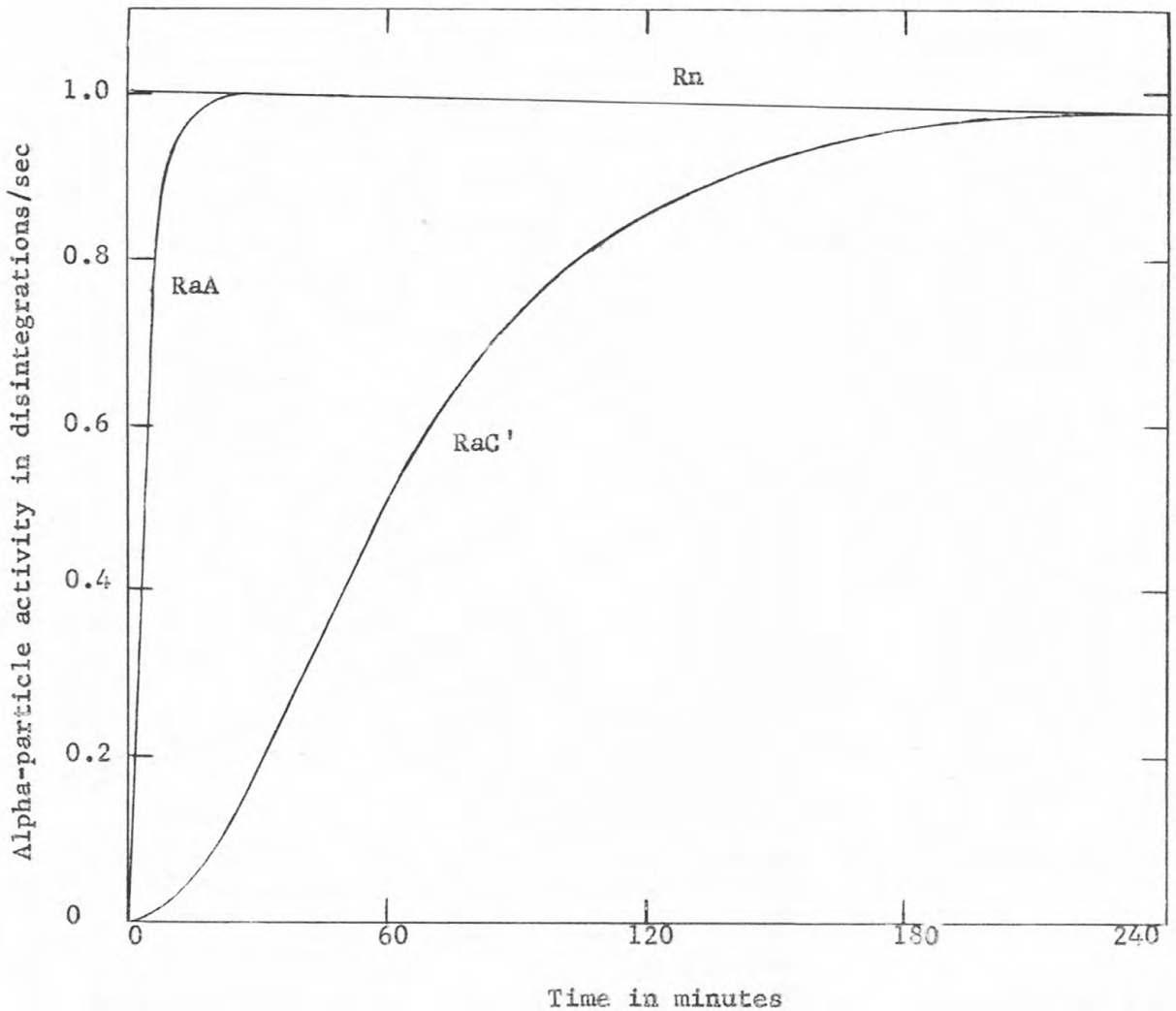

FIGURE 7.- Alpha-particle activity of Rn, RaA, and RaC' at time t after introduction of a unit activity source of Rn into an ionization chamber (after Evans, 1955).

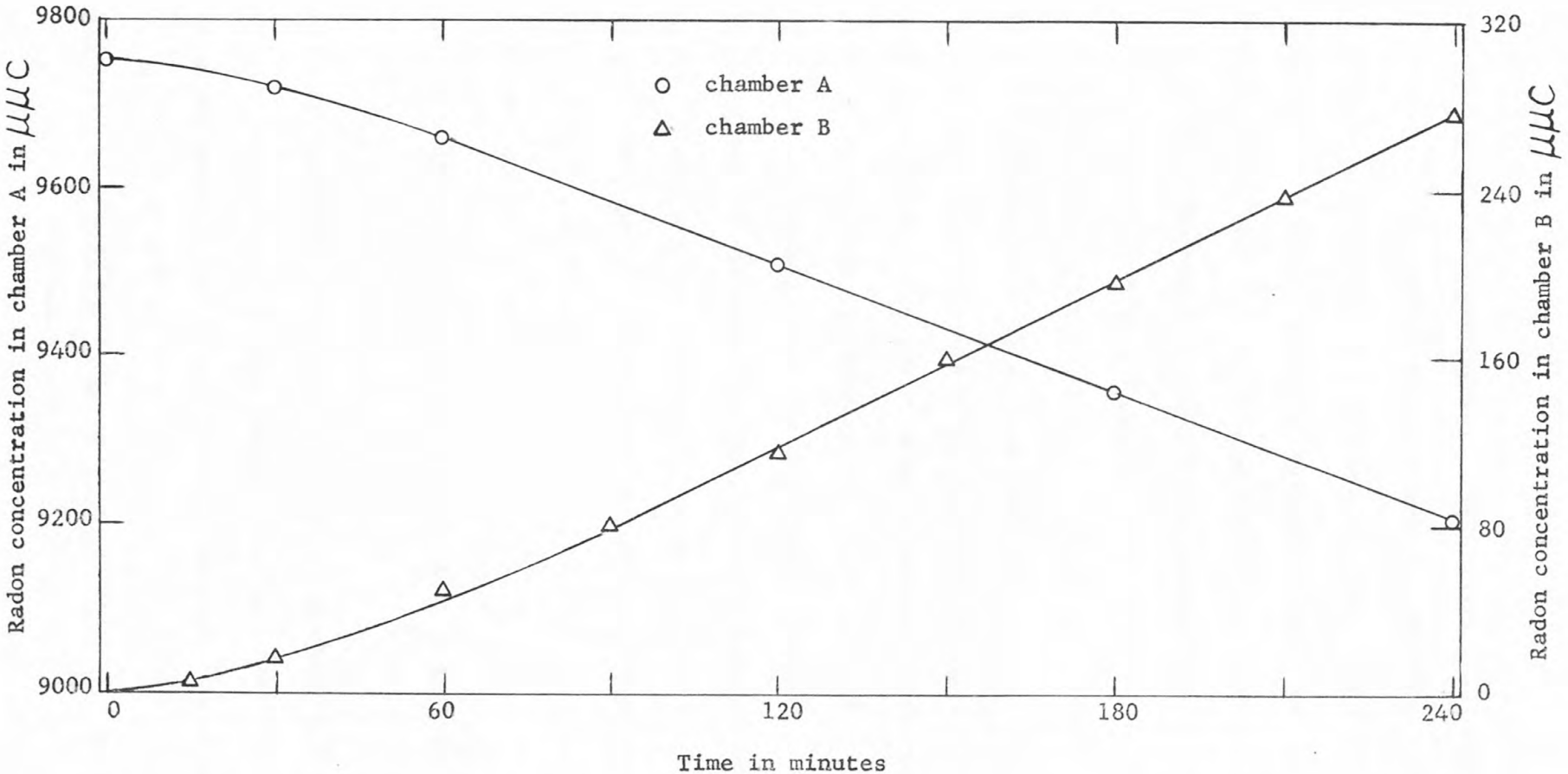

FIGURE 8.- Radon concentration in source chamber (A) and in receiving chamber (B) at time t after diffusion begins.

percent less than the equilibrium concentrations, depending on the core used in the run. In chamber A, and recorded concentrations exceeded the equilibrium concentrations by a maximum of about four percent.

To compensate for nonequilibrium conditions in the chambers, an equilibrium factor (f) was determined empirically such that the product of the recorded concentration and the equilibrium factor would yield the equilibrium concentration. The factor f was obtained by plotting the ratio of the activity of Rn + RaA + RaC' at time t to the equilibrium activity for a unit activity of pure radon introduced into a chamber at t = o. The resulting curve is shown in figure 9.

The curve of figure 9 can be divided into time intervals Δt and the average fraction of equilibrium for these intervals can be determined from the curve. Assuming that the quantity of radon entering chamber B during the time Δt is constant, the equilibrium fractions corresponding to each Δt interval can be summed to give the fraction of equilibrium existing at any time t. Thus, if q is the quantity of radon entering chamber B during the time interval Δ t, and F $(t + \Delta t/2)$ is the average equilibrium fraction at time t,

$$q \Delta t \, H_i = \sum_{i=o}^{t} q \Delta t \, F\left(t_i + \frac{\Delta t}{2}\right) \text{ or } H_i = \sum_{i=o}^{t} F\left(t_i + \frac{\Delta t}{2}\right). \quad (9)$$

If the recorded quantity of radon entering chamber B during an interval Δt is p, the quantity in the chamber at time t would be $\sum_{i=1}^{t} P_i \Delta t$. The recorded quantity and the equilibrium quantity are related by

$$q \Delta t \, H_i = p t \, \Delta t \quad (10a)$$

so that

$$q = p t / H_i = f p . \quad (10b)$$

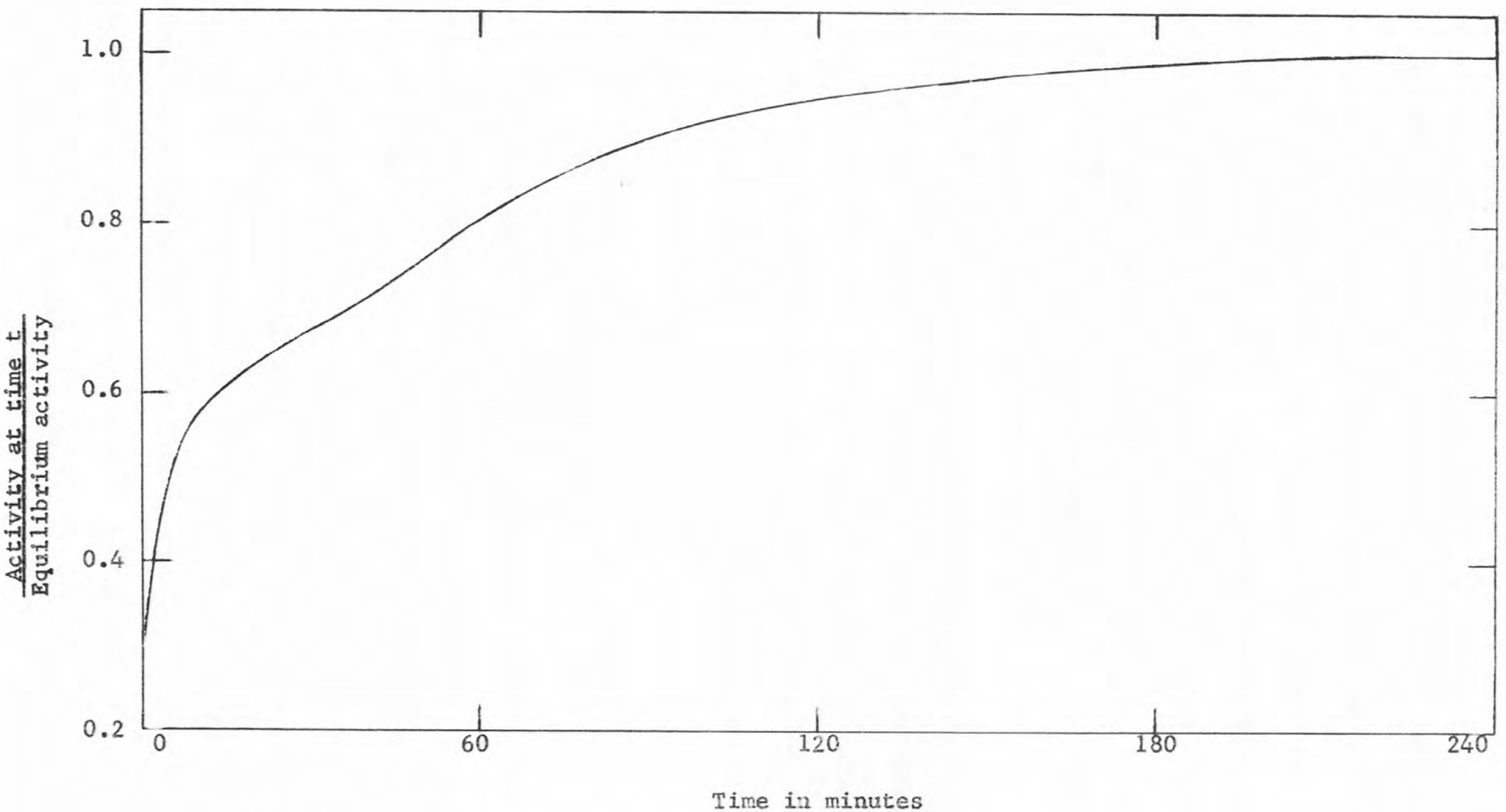

FIGURE 9.- Ratio of the α-particle activity of Rn + RaA + RaC' at time t after introduction of a Rn source into an ionization chamber to the α-particle activity of Rn + RaA + RaC' in equilibrium.

For an interval $\Delta t = 60$ sec the equilibrium fraction at the end of two minutes (from fig. 9) is $H_2 = 0.320 + 0.377 = 0.697$ and $q = 2p/H_2 = 2.87\ p$. In this case $f = 2.87$. Equation (3a) shows that assuming q to be constant is not strictly valid, but the curve representing the changes in radon content in chamber B (fig. 8) indicates that during the first four hours the deviation from linearity is not excessive. In most diffusion runs, the change in radon content in chamber B was essentially constant during the first eight hours of the run.

The initial concentration difference between the two chambers is known absolutely and the equilibrium concentration in chamber B at time t can be obtained from equation (10b). It was determined experimentally that the difference in radon concentration between the two chambers at time t could be obtained, with an average error of less than one percent, from the expression

$$\Delta C_t = (C_o - f C_t) e^{-\lambda t} - f C_t = C_o e^{-\lambda t} - f C_t (1 + e^{-\lambda t}) \quad (11)$$

where C_o is the initial concentration in chamber A, C_t is the recorded concentration in chamber B at time t, f is the equilibrium factor at time t, and λ is the decay constant of radon (2.08×10^{-6} sec^{-1}).

Since the initial concentration in chamber B is always zero, the difference in concentration between the two chambers at $t = 0$ is just the initial concentration in chamber A, or $\Delta C_o = C_o$.

From the relations developed in this section, the apparent diffusion coefficient for any diffusion run can be evaluated by substituting $\Delta C_o / \Delta C_t$ the length and area of a particular core, the volumes of the two chambers, and the diffusion time in equation (8).

EXPERIMENTAL RESULTS

Factors influencing the permeability of artificial sandstone cores

Because mathematical equations relating permeability to such factors as cement content, grain size, and porosity are not easily obtained, the experimental results are presented in the form of curves.

In order to relate porosity and permeability, a series of cores were constructed using sand of medium grain size and Grefco cement. A range of porosities were obtained for cores containing 10, 15, 20, 25, 32.5, and 40 percent cement. Figures 10, 11, 12, and 13, are plots of the permeability of these cores as a function of porosity. The least square curves of the form $K = \alpha C^{\beta\Phi}$ are plotted with the experimental data. In these equations, Φ is the fractional porosity, K is the permeability in millidarcys, and α (cm^2) and β (non-dimensional) are parameters that are functions of the cement content and the grain size of the cores. A similar relation between permeability and porosity has been obtained for samples of natural sandstone (Paine, 1956). The slopes of these curves tend to increase between 40 percent cement content and 20 percent cement content, but decrease rapidly between 20 percent and 10 percent cement content. Apparently, a cement content of 20 percent is very nearly the transition point between "floating" grains and grain to grain contacts. The grains in cores containing less than 20 percent attain an increasing number of grain contacts as the cement content decreases and fracturing of the grains during the construction process probably results in a larger number of blocked passages. The higher pressures required to obtain porosities of

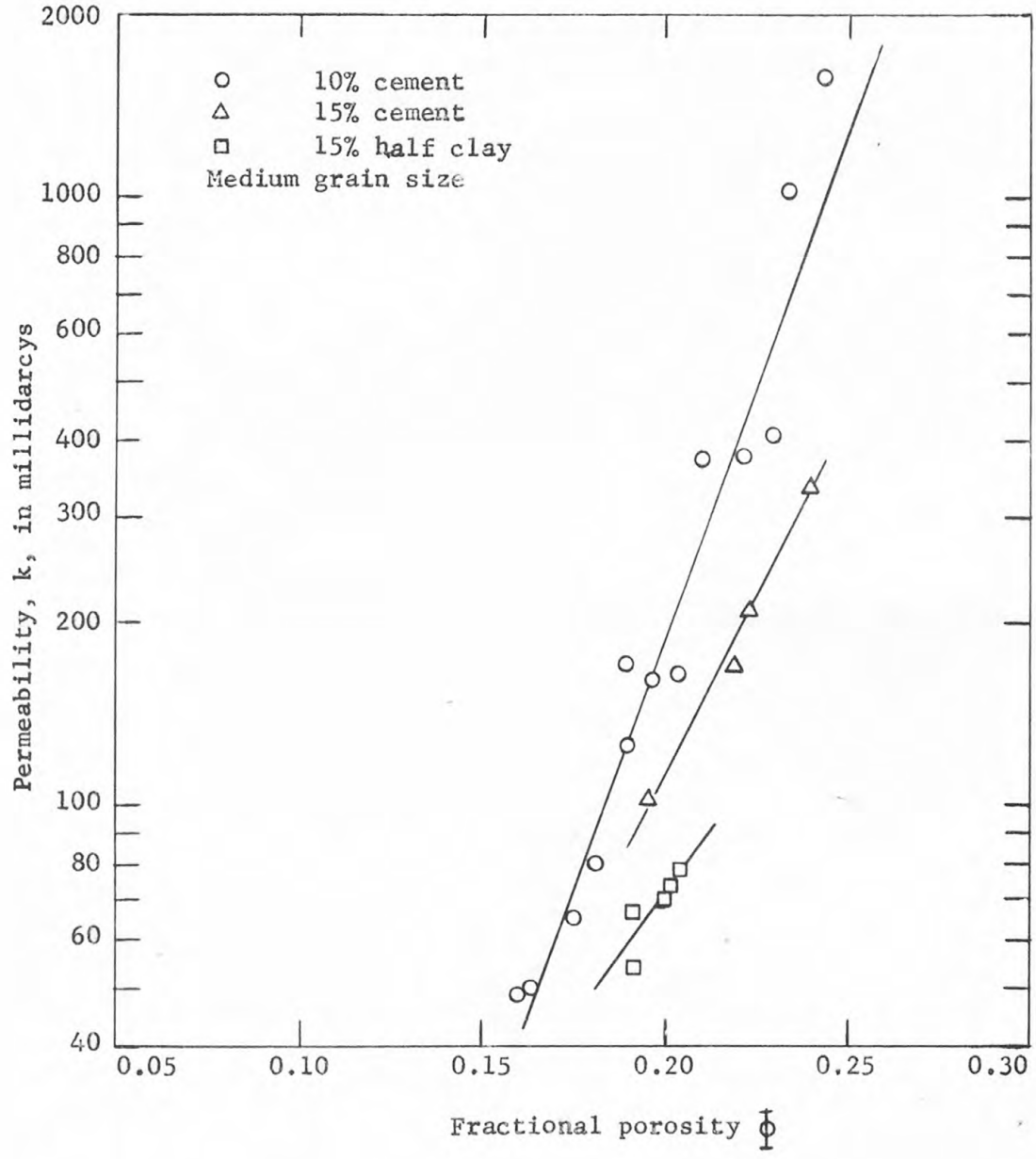

FIGURE 10.- Core permeability versus core porosity for artificial sandstone cores of medium grain size containing 10 percent cement, 15 percent cement, and 15 percent cement (half Grefco, half clay).

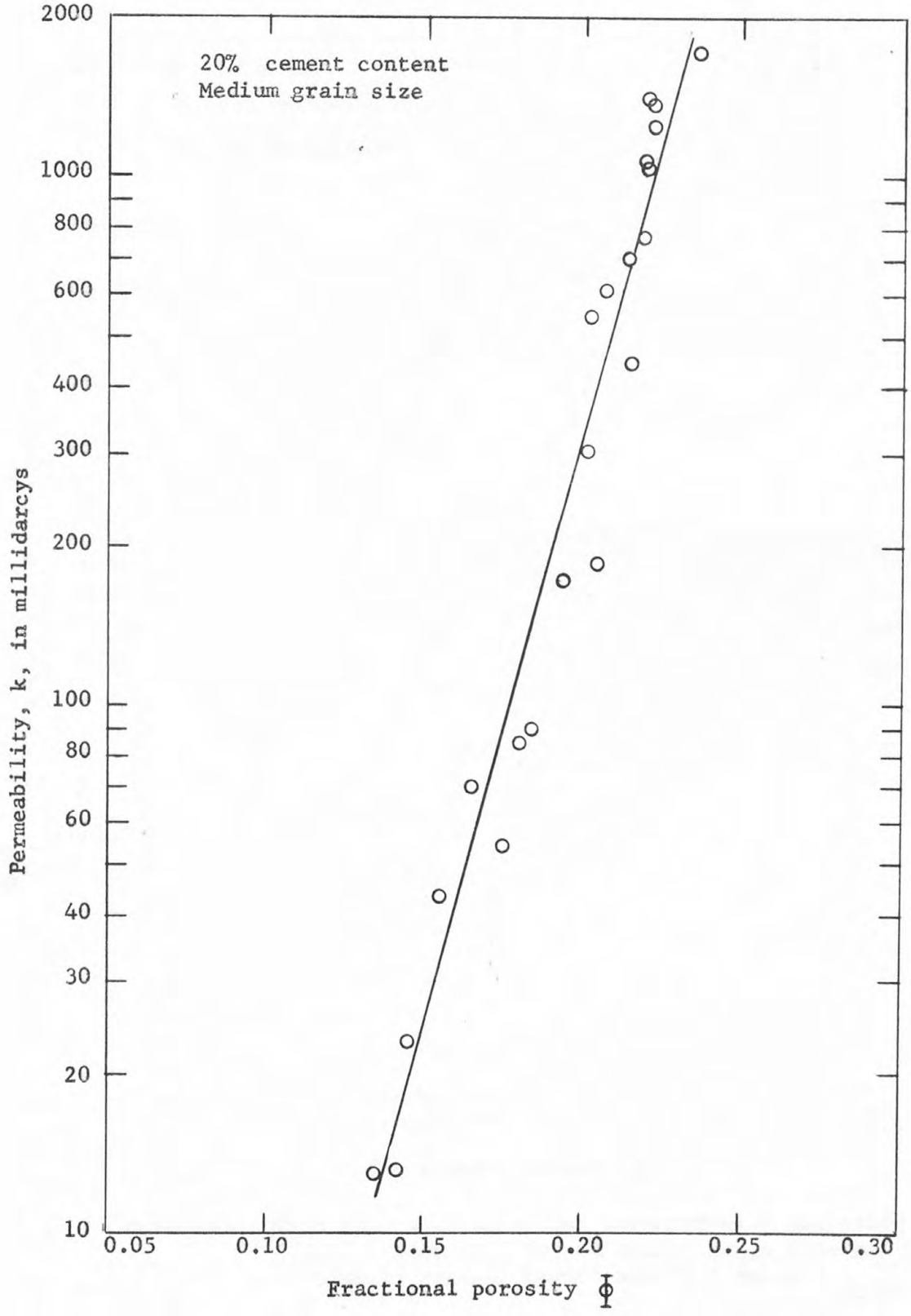

FIGURE 11.- Core permeability versus core porosity for artificial sandstone cores of medium grain size containing 20 percent cement.

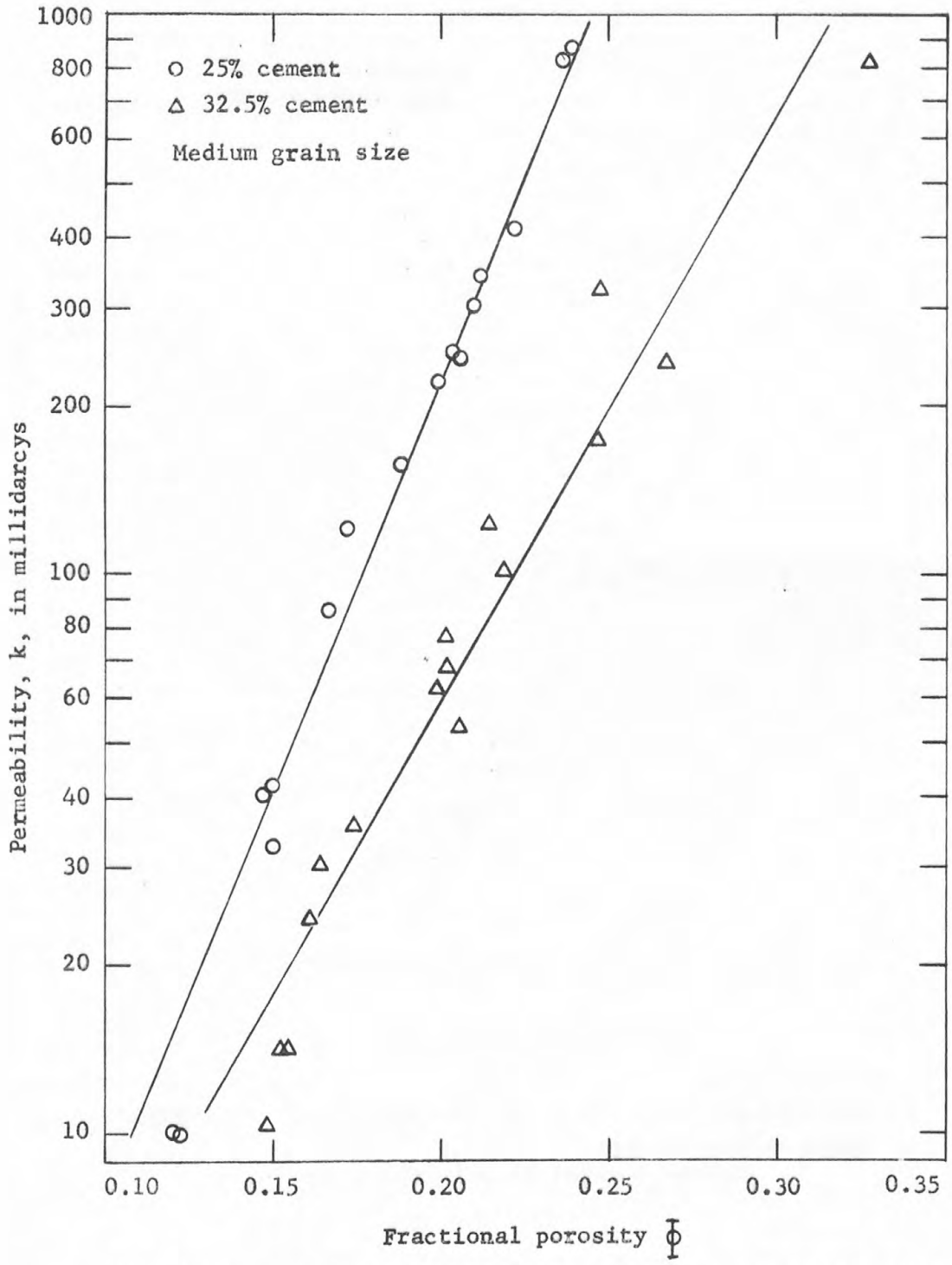

FIGURE 12.- Core permeability versus core porosity for artificial sandstone cores of medium grain size containing 25 percent cement and 32.5 percent cement.

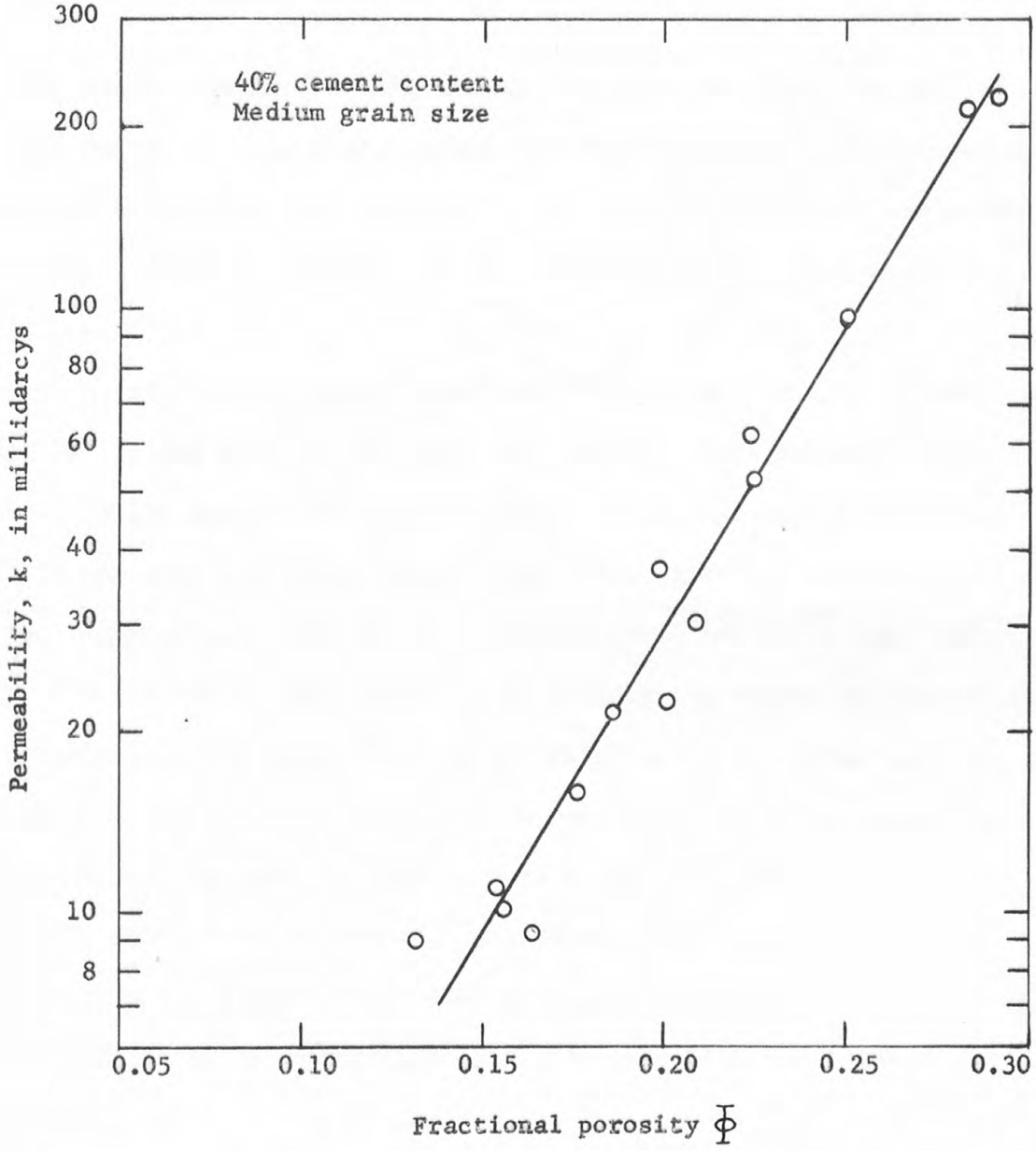

FIGURE 13.- Core permeability versus core porosity for artificial sandstone cores of medium grain size containing 40 percent cement.

the same range as those found in higher cement contents tend to compact the small amount of cement that is present more firmly between the grains so that the permeability is decreased. In natural unfractured sandstones, high permeabilities are normally associated with large pore space (Fancher, 1933).

The curves for 40 percent cement and 32.5 percent (figure 12 and figure 13) are not widely divergent, and, in fact, have essentially the same slope indicating that in this cement range the sand grains have little effect on the effective pore space of the core. Although the permeability of cores containing relatively large quantities of cement is due, effectively, to the permeability of the cement, it is largely the degree of compaction that determines the slope of the curve. Slightly greater construction pressures are required to obtain a given porosity for a core containing 32.5 percent cement than are necessary to produce the same porosity in a core of 40 percent cement content. All curves converge for low values of porosity, and for porosities below about 13 percent the permeability does not vary widely except in the 15 percent and 10 percent cement curves.

Data for cores composed of 10 percent cement were difficult to obtain using the available equipment. It was not possible to construct such cores with porosities less than about 19 percent. The cores of higher porosity were easily constructed, but cores of porosity greater than about 21 percent were not rigid enough to withstand the sealing process. During the heating process, the liquid lucite, under pressure, readily moved into the pore spaces of the more porous cores, and due to contraction on cooling, carried the encroached portion of the core away from the center

of the core. As a result of this movement a small cylinder of core remained unsupported and the core would tend to disintegrate.

A comparison of permeability-porosity curves for the cores of 15 percent cement content (all Grefco), and for cores containing 15 percent cementing material composed of half Grefco and half kaolin is shown in figure 10. The effect of the clay is to decrease the permeability at a particular porosity. It appears that the clay absorbs and holds more moisture from the air resulting in a larger percentage of blocked pore spaces and a reduction in permeability. However, the cores containing clay fit the same type of curve as the Grefco cores.

Although the composition of the cores was controlled in construction, considerable scatter of points occurred in the permeability-porosity curves. Undoubtedly, the use of a grain range rather than a uniform grain size contributed to the scatter. It is probable that the ratio of large to small grains varied in samples that were considered to be of the same grain size, and the sand taken from the supply, even though sieved, would not contain the same ratio of large to small grains each time.

In addition, permeability determinations are especially sensitive to small changes in core area and length. Often it was difficult to measure accurately the core diameter due to encroachment of the lucite, and determination of core length was hindered by the uneven nature of the core face. In order to minimize errors, core dimensions used in determining the permeability were the average of 12 to 15 readings.

Although difficult to evaluate, a third source of error occurs in mixing the sand and cement before pressing. Obviously, the packing of the smaller grains could have an influence on the permeability. Even

carefully mixed cement-sand mixtures showed some evidence of aggregation, and in some instances the cement content was greater at one end of a core due to settling. Whenever possible such cores were discarded, or cut so that the area of accumulation was eliminated.

Finally, errors due to porosity determinations contribute to the scatter. The method of determining effective core porosity by water flooding is far from satisfactory. Evaporation occurs when the core is weighed wet, and absorption of moisture from the air causes variations in the dry weight. Three to four porosity determinations were carried out for each core, and an average value selected as the effective porosity. Changes of porosity of 1/2 to 1 1/2 percent porosity were noted for some cores between the first and the last porosity determination. Errors in core diameter and length also enter into porosity computations.

The effect of compaction is clearly indicated in figure 14 in which core permeability is plotted as a function of cement content. The porosity of each core is approximately 20 percent and all cores are composed of the same grain size (medium). The transition point between cores with a large number of grain to grain contacts and cores in which the grains are largely "floating" occurs at approximately 20 percent cement content. The increased compaction of the cement and the increased number of grain contacts, sharply reduces the permeability of cores containing less than 20 percent cement. A plot of construction pressure versus cement content for the set of cores in figure 14 aids in pointing out the influence of compaction on both permeability and porosity. An attempt was made to fit a polynomial of least order to the points in figure 14, but the data were too few to provide an equation. The results

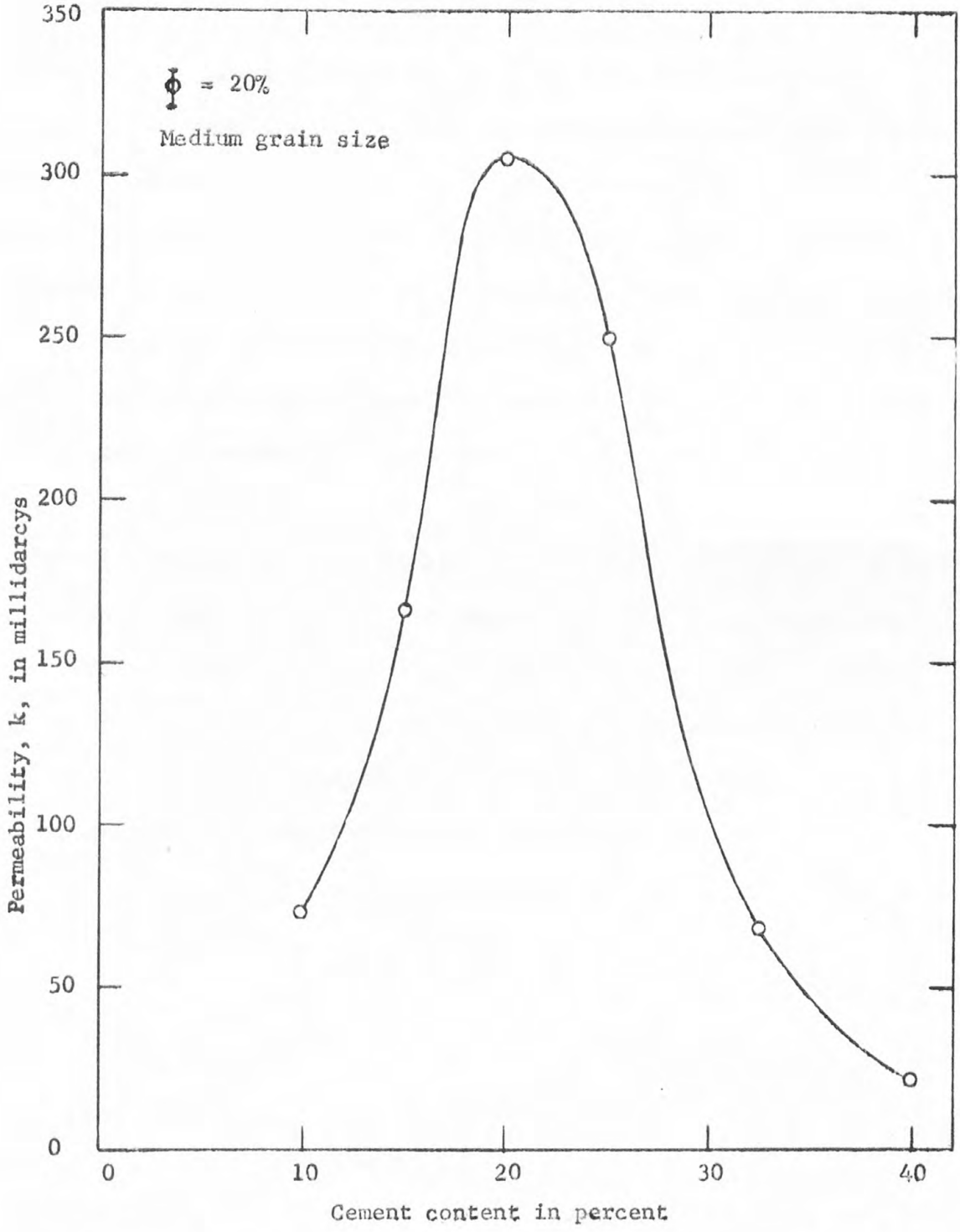

FIGURE 14.- Core permeability versus cement content of artificial sandstone cores of medium grain size and 20 percent porosity.

indicate that such a polynomial would be of order greater than 4.

Figure 15 shows the increase in construction pressure necessary to produce cores of the same porosity as the cement content is decreased. The higher construction pressures required for the cores of low cement content probably contribute greatly to the observed reduction in permeability.

The relationship obtained between permeability and mean grain size for each grain size range is shown in figure 16. The porosity of each core is about 20 percent and the cement content of each core is 15 percent.

A least square fit of an equation of the form $k = \gamma g^{\sigma}$ (g is the mean grain diameter in cm, k is the permeability in millidarcys, and γ and σ are functions of the core porosity and cement content) yields a value of σ of 2.08 for the cores of 15 percent cement content. This value of σ is in good agreement with the predicted value of 2 for a uniform grain size (Wyckoff and others, 1934).

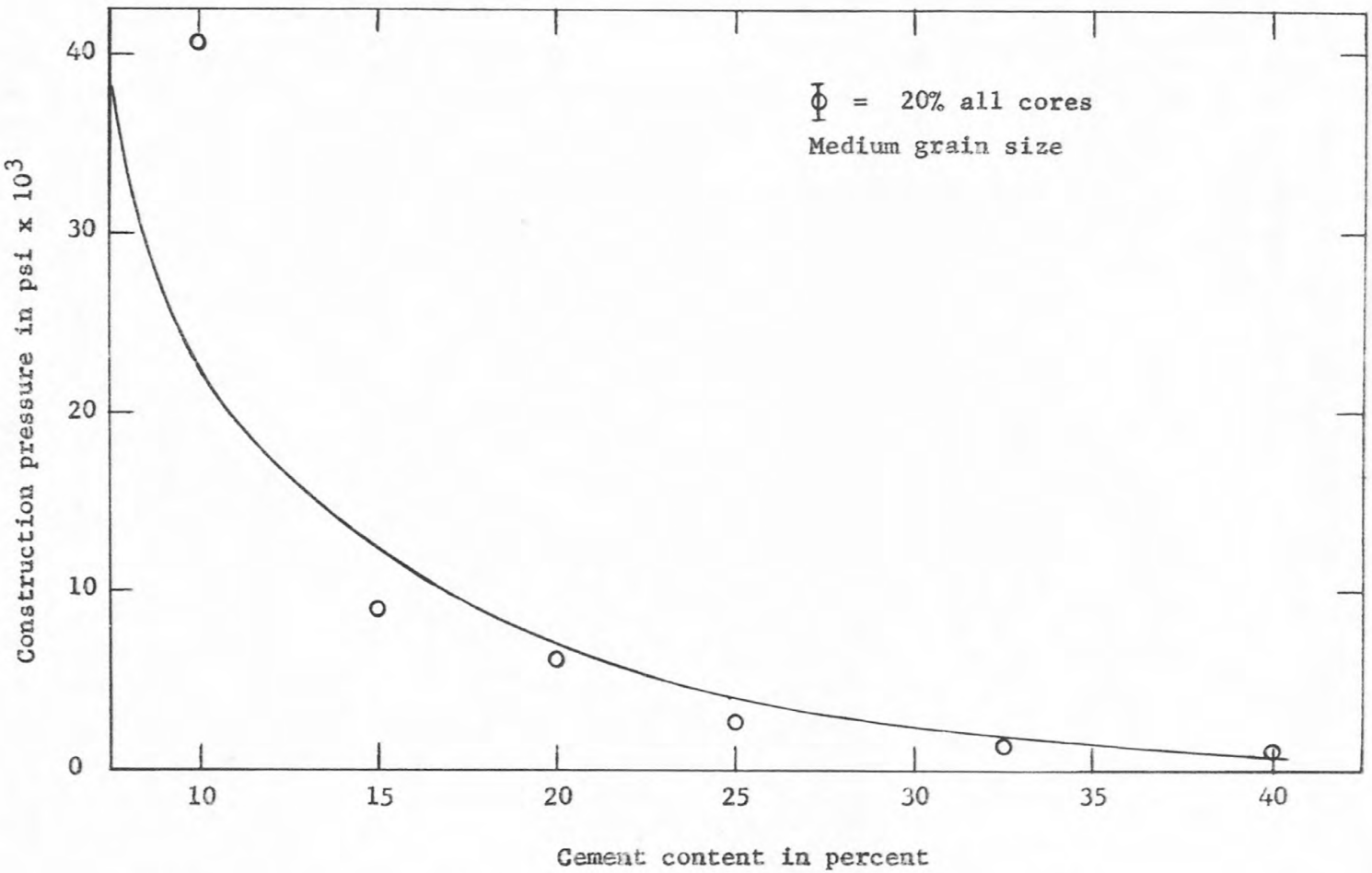

FIGURE 15.- Construction pressure required to produce a core of 20 percent porosity with a particular cement content.

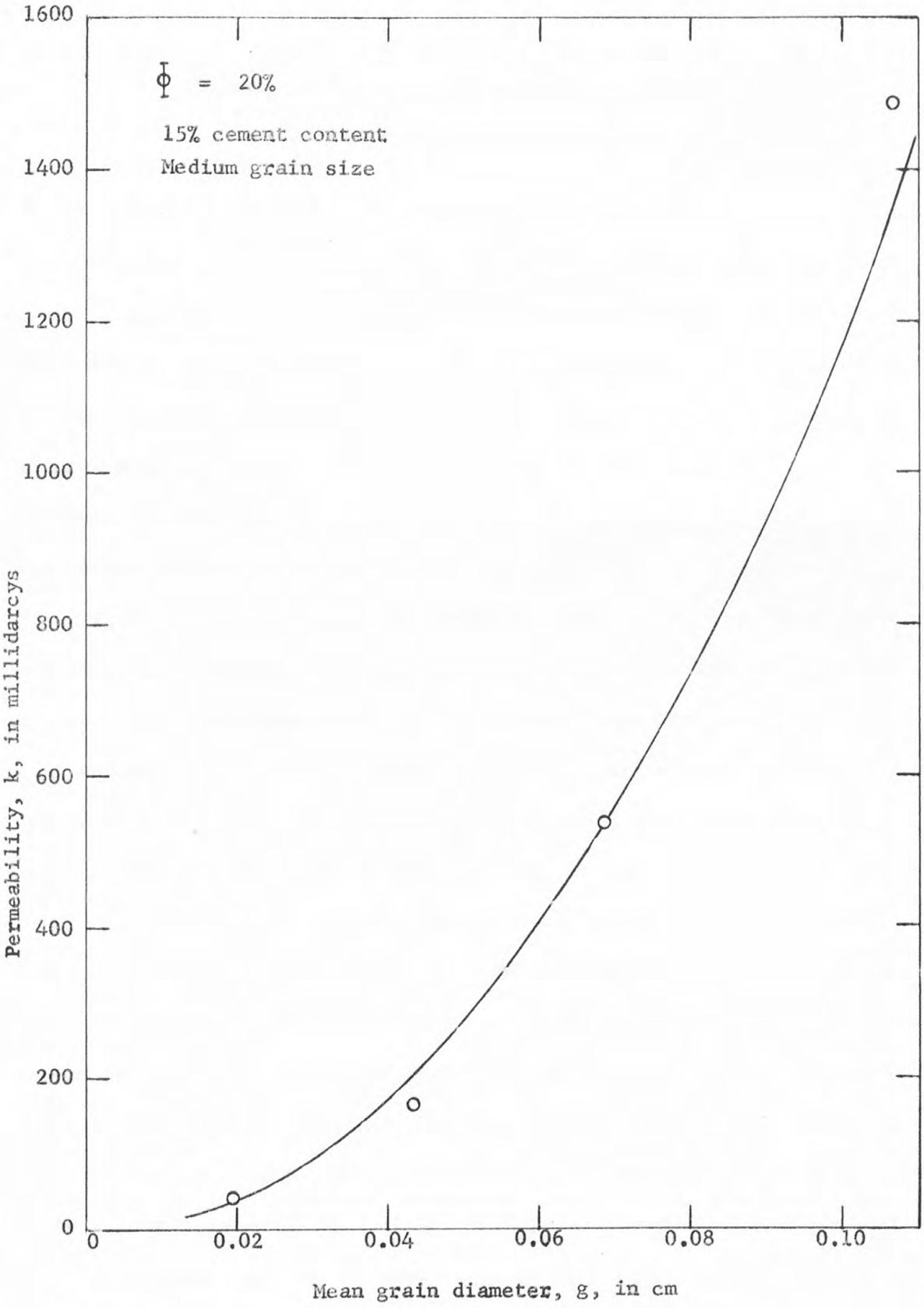

FIGURE 16.- Core permeability versus mean grain diameter of artificial cores of 20 percent porosity and 15 percent cement.

Relation between apparent diffusion coefficient and core characteristics

The apparent diffusion coefficients were measured for three series of artificial sandstone cores that varied in porosity, grain size, and cement content. For the first series (the cores of fig. 14), each core had the same porosity and grain size but different cement contents. For the second series (the cores of 15 percent cement of fig. 10), each core had the same grain size and cement content but different porosity. For the third series (the cores of fig. 16), each core had the same porosity and cement content but a different mean grain size.

Figure 17 is an example of the method used to correct the apparent diffusion coefficients obtained using the original diffusion system to the apparent diffusion coefficients for four cores measured in the modified diffusion system. The porosity and the grain size of each of these cores is the same but the cement content is different (the cores of fig. 14) containing 15 percent, 20 percent, 25 percent, and 40 percent cement).

In figure 17a, the apparent diffusion coefficients of these four cores, measured in both the original and the modified diffusion systems, were plotted as a function of the core length. A least mean square curve (assuming a straight line) was drawn through each of the two sets of data points. The apparent diffusion coefficient of all the cores of this series measured in the original diffusion system were then plotted as a function of core length as shown in figure 17b. The difference between the two least mean square curves at a particular core length was then added to the apparent diffusion coefficient of the cores which were measured only in the original diffusion system in order to obtain an apparent diffusion coefficient corresponding to a measurement in the modified system.

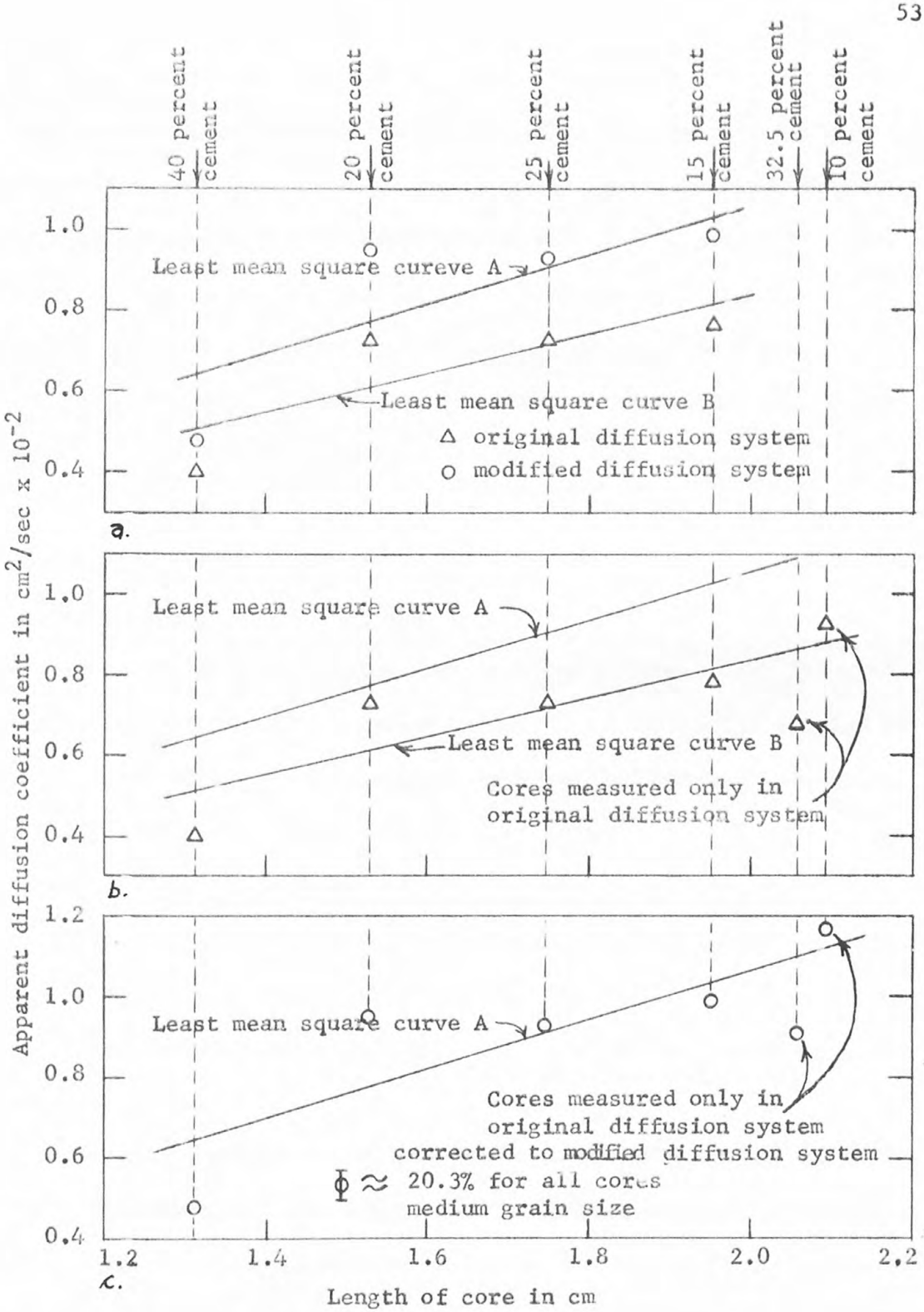

FIGURE 17.- Example of method of correcting apparent diffusion coefficients of original diffusion system for diffusion in the connecting tubing.

The final curve of the corrected apparent diffusion coefficients measured in the modified system is shown in figure 17c. In this series, it was necessary to correct only two additional cores. The apparent diffusion coefficients of the cores of each of the three core series measured only in the original diffusion system were corrected as described above.

The effect of cement content on the apparent diffusion coefficient of radon (for cores of the same porosity and grain size), is shown in figure 18. The apparent diffusion coefficients plotted in figure 18 were obtained for the modified diffusion system by the method described above (fig. 17c), and, for comparison, the apparent diffusion coefficients measured in the original diffusion system are also shown. For the modified system, a gradual, almost linear, increase in apparent diffusion coefficient occurs with decreasing cement between 32.5 percent cement and 20 percent cement. For cement contents less than 20 percent, the apparent diffusion coefficient increases sharply to a maximum value at the lowest cement content available (10 percent). The apparent diffusion coefficient decreases sharply for cement contents greater than 32.5 percent and the minimum apparent diffusion coefficient occurs at a cement content of 40 percent.

Although it is probable that some radon is adsorbed on the cement of the core, adsorption alone should result in a linear change in apparent diffusion coefficient as a function of cement content because the amount of adsorption is proportional to the surface area of the cement. If adsorption is negligible, the larger apparent diffusion coefficients corresponding to cores of cement contents less than 20 percent is probably due to a greater number of pore spaces available to the diffusing gas.

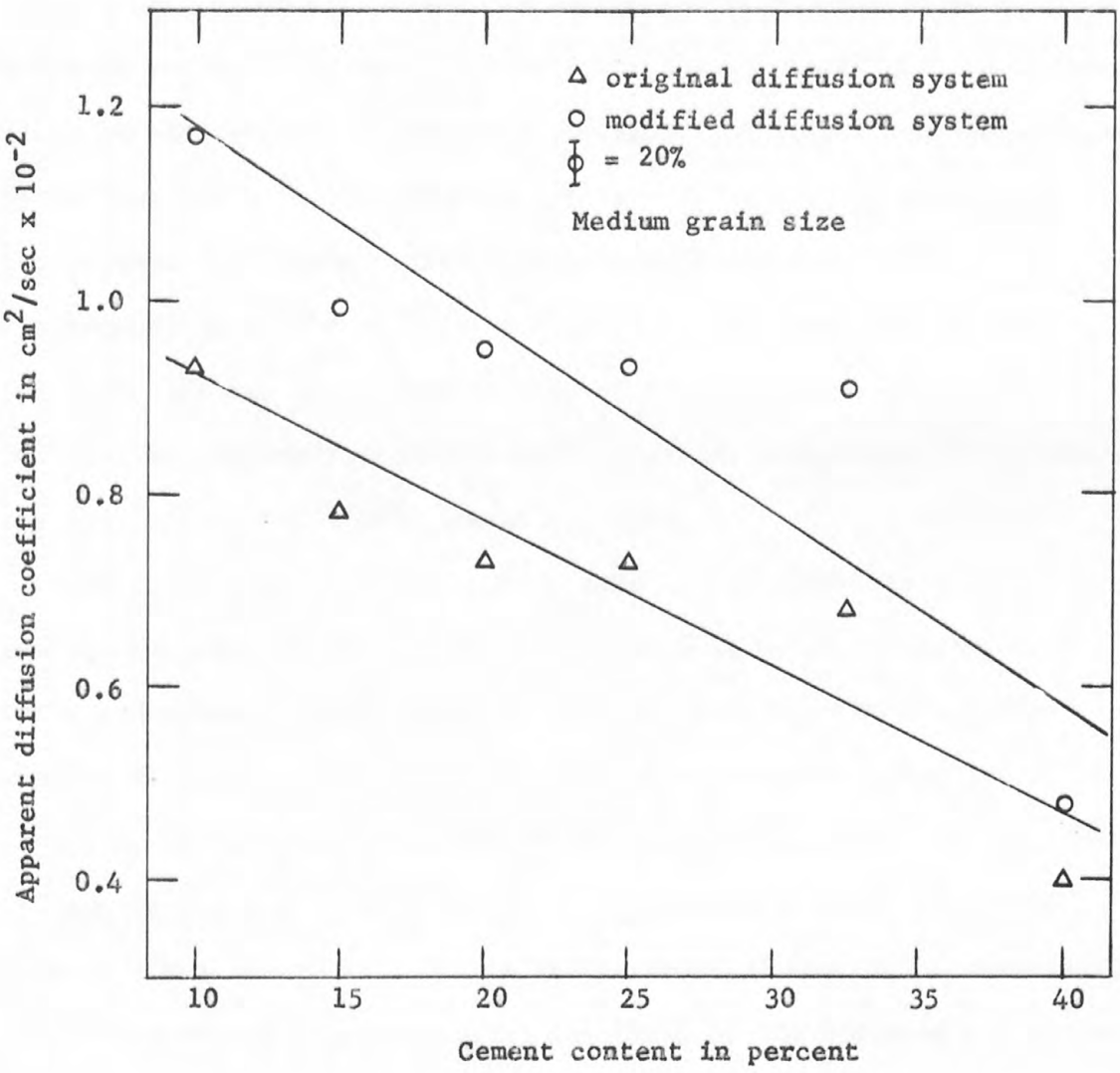

FIGURE 18.- Apparent diffusion coefficient versus cement content for cores of 20 percent porosity and medium grain size, showing original diffusion system data and modified diffusion system data.

The apparent diffusion coefficients for the original diffusion system follow about the same trend as those determined in the modified system except that in the original diffusion system the apparent diffusion coefficients for 15 percent cement and 20 percent cement are slightly lower relative to the apparent diffusion coefficients for cores of 25 percent and 32.5 percent cement. Although a straight line (least mean square) was drawn through the data of figure 18, it is obvious that no simple relation exists between the apparent diffusion coefficient and the cement content.

A comparison of the apparent diffusion coefficients for the modified system (fig. 18) and the permeabilities of the same cores (fig. 14) illustrates that the apparent diffusion coefficient is independent of permeability for cores of different cement contents.

Assuming that in the absence of a core in the diffusion system the true diffusion coefficient of radon in argon (D_o) would be measured (Garrels and others, 1949), equation (8) can be used to obtain the effective area (A'), the ratio of the effective length to the effective area (A'/L'), the effective directional porosity ($A'L/AL'$), or the lithologic factor ($\Phi/(A'L/AL')$). In these terms A and L are the area and length and Φ is the porosity of the core. The ratio A'/L' is obtained by substituting the ratio of the measured concentration differences ($\Delta C_o/\Delta C_t$) and the true diffusion coefficient of radon in argon in equation (8) so that for a particular core

$$\frac{A'}{L'} = \frac{V}{2\,t\,D_o} \ln \frac{\Delta C_o}{\Delta C_t} \qquad (12)$$

where D_o is taken as 0.115 cm^2/sec at a temperature of 26° C and a pressure of 650 mm (Hirst and Harrison, 1938-1939).

Then, assuming that the measured length of the core (L) and the effective length (L') are equal, the effective area (A') can be obtained from the product of the A'/L' ratio and L or

$$\frac{A'}{L'} L = A'. \tag{13}$$

The effective directional porosity and the lithologic factor can be obtained easily when A'/L' is known.

The lithologic factor, plotted as a function of core cement content, is shown in figure 19 for the cores of figure 14. The lithologic factors are essentially constant for cement contents between 10 percent and 32.5 percent, but for 40 percent cement the lithologic factor increases sharply. The values of the lithologic factor plotted in figure 19 are in excellent agreement with those reported by Klinkenberg (1951) for consolidated sandstones.

The apparent diffusion coefficients of the cores of figure 10 (medium grain size and 15 percent cement content, but having a range of porosities) are shown in figure 20 as a function of the core porosity. Except for the cores of 19.7 percent, 23.3 percent, and 24.3 percent porosity, the apparent diffusion coefficient increases almost linearly with increasing porosity. It is difficult to account for the deviation of these three cores from the general trend since the maximum variation in the apparent diffusion coefficient determined from three separate diffusion runs with each of these cores was about three percent.

Neglecting the cores mentioned above, the general trend of the plot of apparent diffusion coefficient versus porosity indicates a non-linear increase in the apparent diffusion coefficient with an increase in core porosity. The scatter of data in figure 20 is such that a quantitative

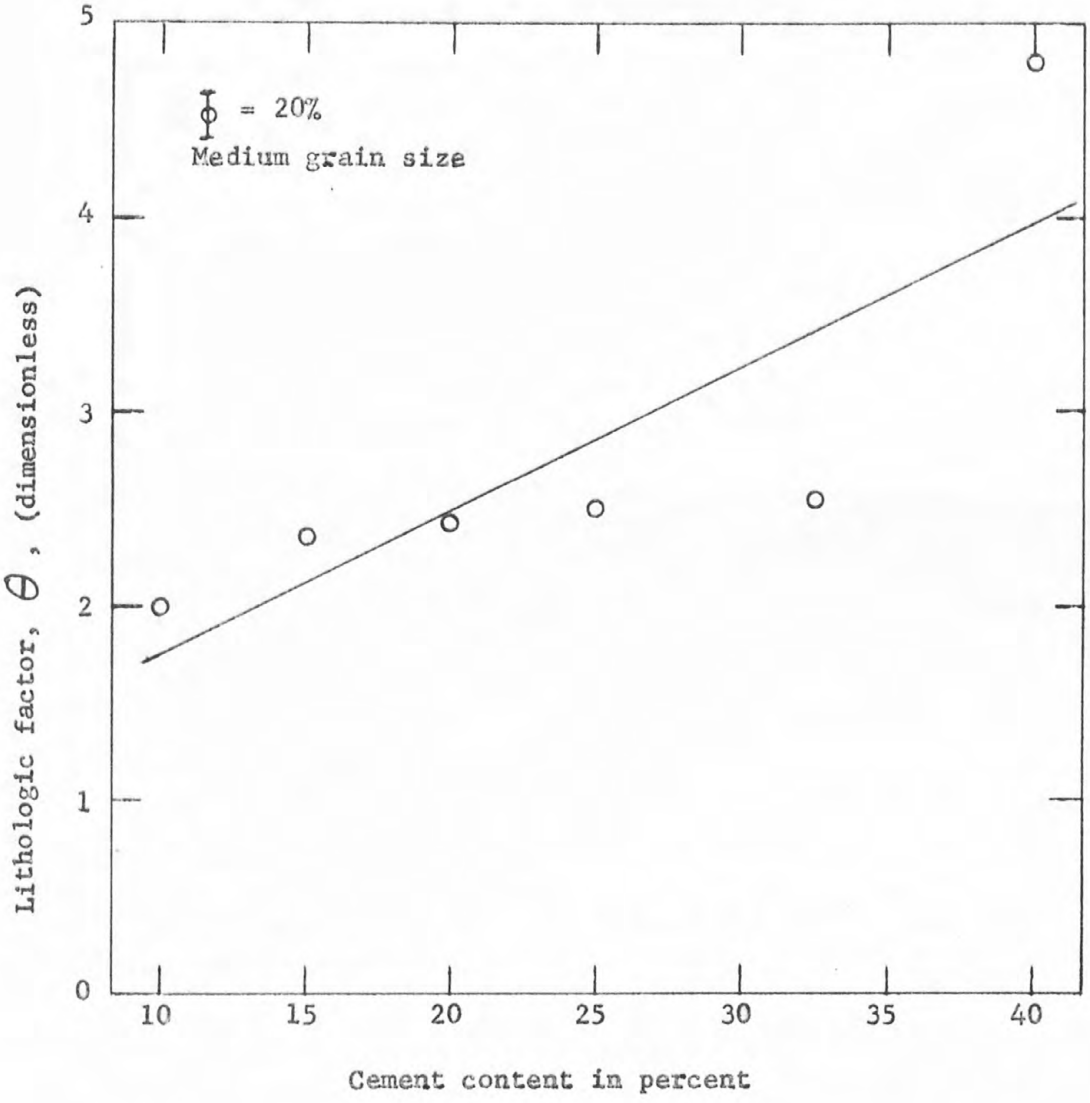

FIGURE 19.- Lithologic factor versus cement content of artificial sandstone cores of 20 percent and medium grain size.

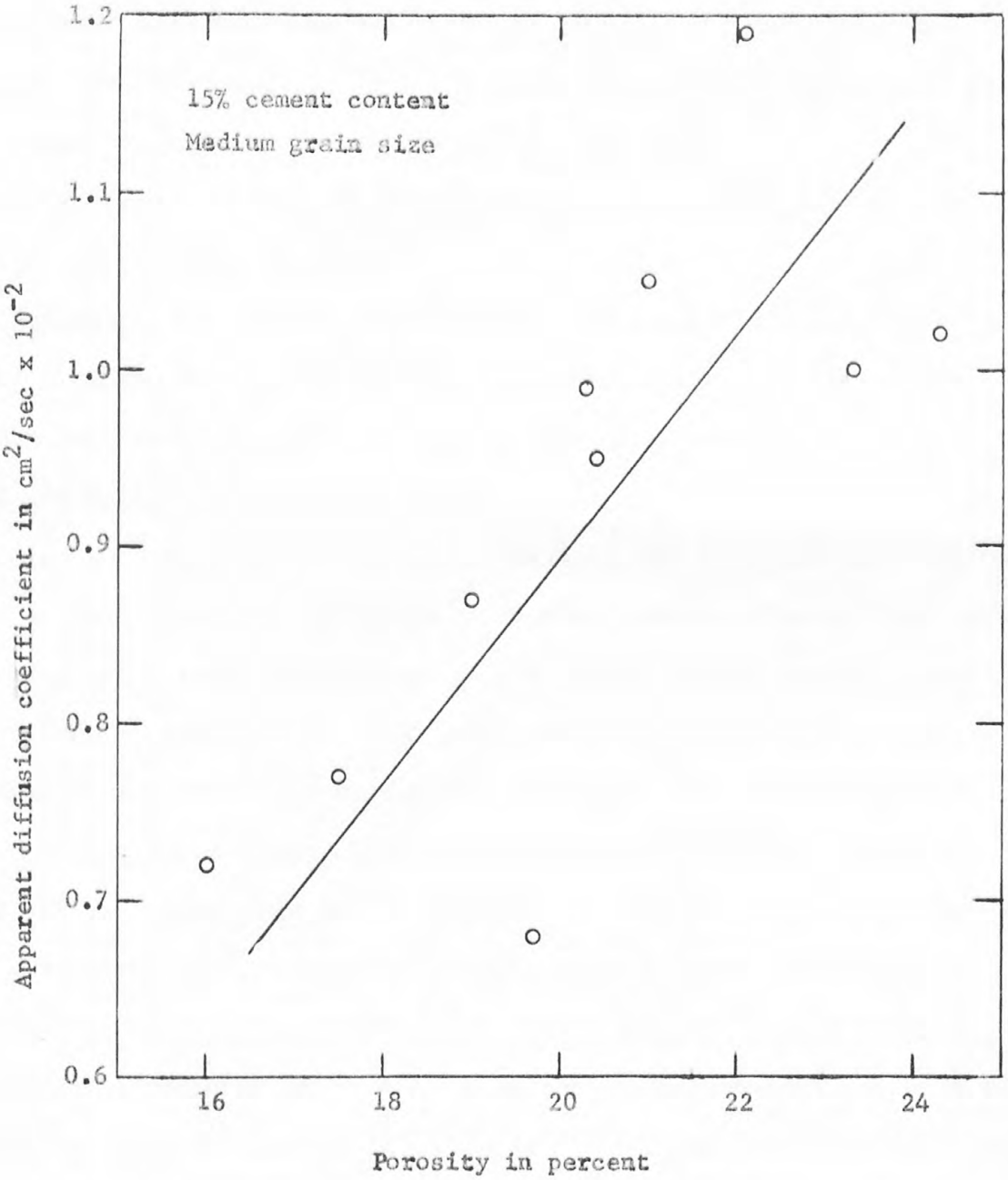

FIGURE 20.- Apparent diffusion coefficient versus core porosity for cores of 15 percent cement and medium grain size.

relation between the apparent diffusion and the core porosity cannot be established. However, from the trend of the data it appears that the apparent diffusion coefficient (D_a) is related to the porosity (ϕ) by an equation of the form $D_a = \psi \phi^{\epsilon} \; (\epsilon > 1)$ where ψ (cm^2/sec) and ϵ (dimensionless) are factors dependent on grain size and cement content.

The least square curve of figure 20, when extrapolated to zero apparent diffusion coefficient, yields a porosity of about six percent. Similar values of intercept porosity have been reported for the diffusion of CS_2 in soil (Blake and Page, 1948).

Figure 21 is a plot of the effective area versus the porosity for the cores of figure 20. The effective areas were obtained from equation (12). The effective area is proportional to the product of the apparent diffusion coefficient and the measured core area so that figure 21 can be obtained directly from figure 20 by multiplying the values for the apparent diffusion coefficient by the measured area of the corresponding core. Figure 21 illustrates that in the cores of 19.7 percent 23.3 percent, and 24.3 percent, the apparent diffusion coefficients (fig. 20) are low because the effective area available to the diffusing gas is low. The effective directional porosities (which are not shown) of the cores of figure 20 increase with increasing porosity in the same manner as the apparent diffusion coefficients of the same cores. In general, the values of the effective directional porosity and the A'/L' ratio are lower for cores yielding smaller diffusion coefficients.

The apparent diffusion coefficients for six cores (the cores of figure 16 with 20 percent porosity and 15 percent cement and three

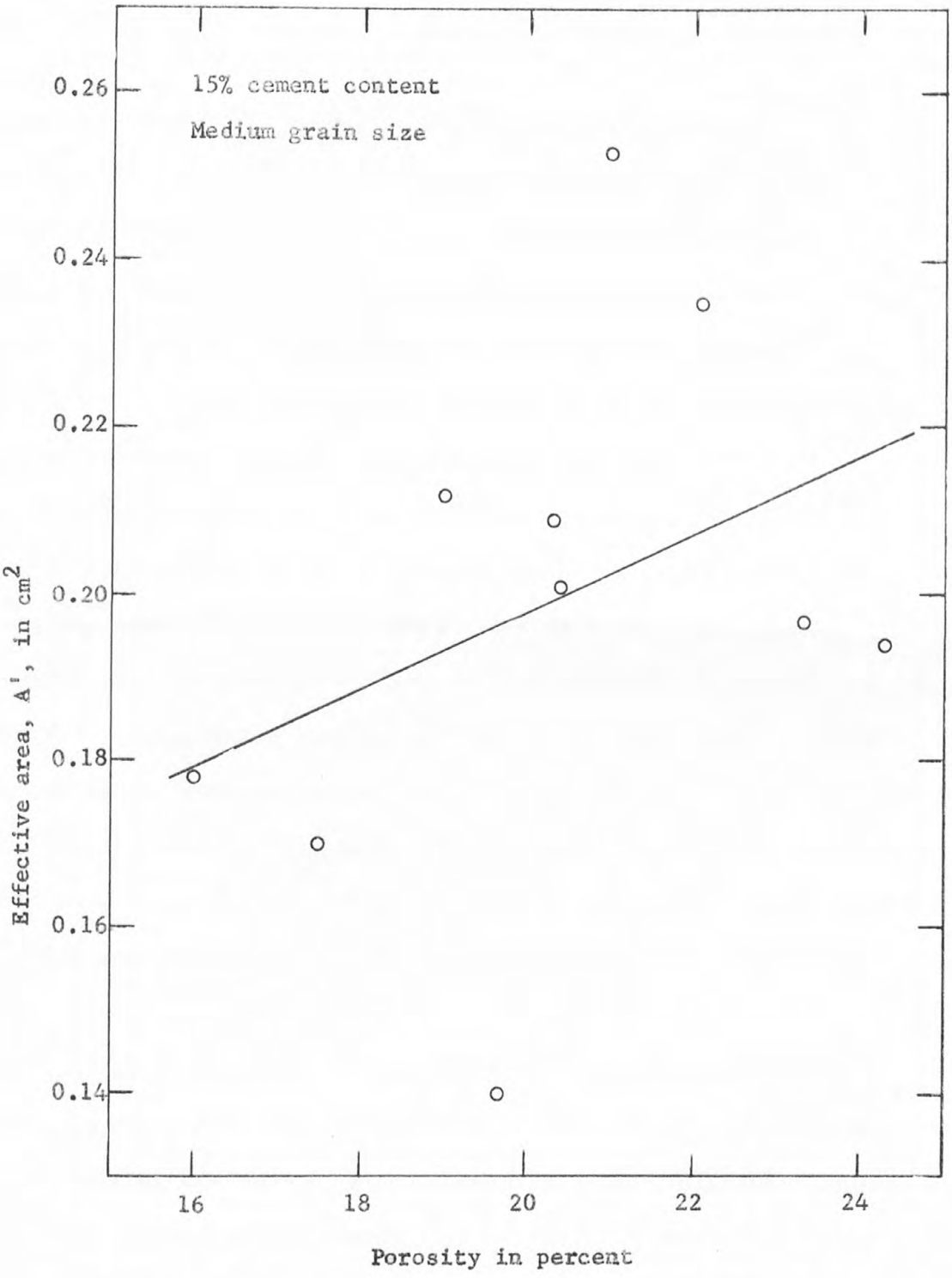

FIGURE 21.- Effective area versus core porosity for artificial sandstone cores of 15 percent cement and medium grain size.

additional cores of 15 percent cement and about 21 percent porosity) containing sand (with average mean diameter of .019 cm, .043 cm, and .069 cm) and two cores containing plastic beads (averaging 0.107 cm in diameter) are plotted in figure 22 as a function of the mean grain diameter. Although the apparent diffusion coefficients plotted for any pair of cores having the same mean grain diameter were not identical, the porosities of these cores were sufficiently close to show the difference in apparent diffusion coefficient for cores constructed to be nearly identical. Because the apparent diffusion coefficient of a particular core was essentially constant in as many as four separate diffusion runs, the difference in apparent diffusion coefficient for each pair of cores representing a particular grain size in figure 22 cannot be attributed to experimental error. The scatter of the data in figure 22 for each pair of cores representing a particular grain diameter probably results from variations in packing of the smaller grains in the individual cores.

The general trend of the data (figure 22) indicates a possible increase in apparent diffusion coefficient with increasing grain size. However, data were not sufficient to establish any clear relationship between the apparent diffusion coefficient and the mean grain size, but it is probable that some relationship could be determined if a larger number of cores of different grain size were available for diffusion measurements.

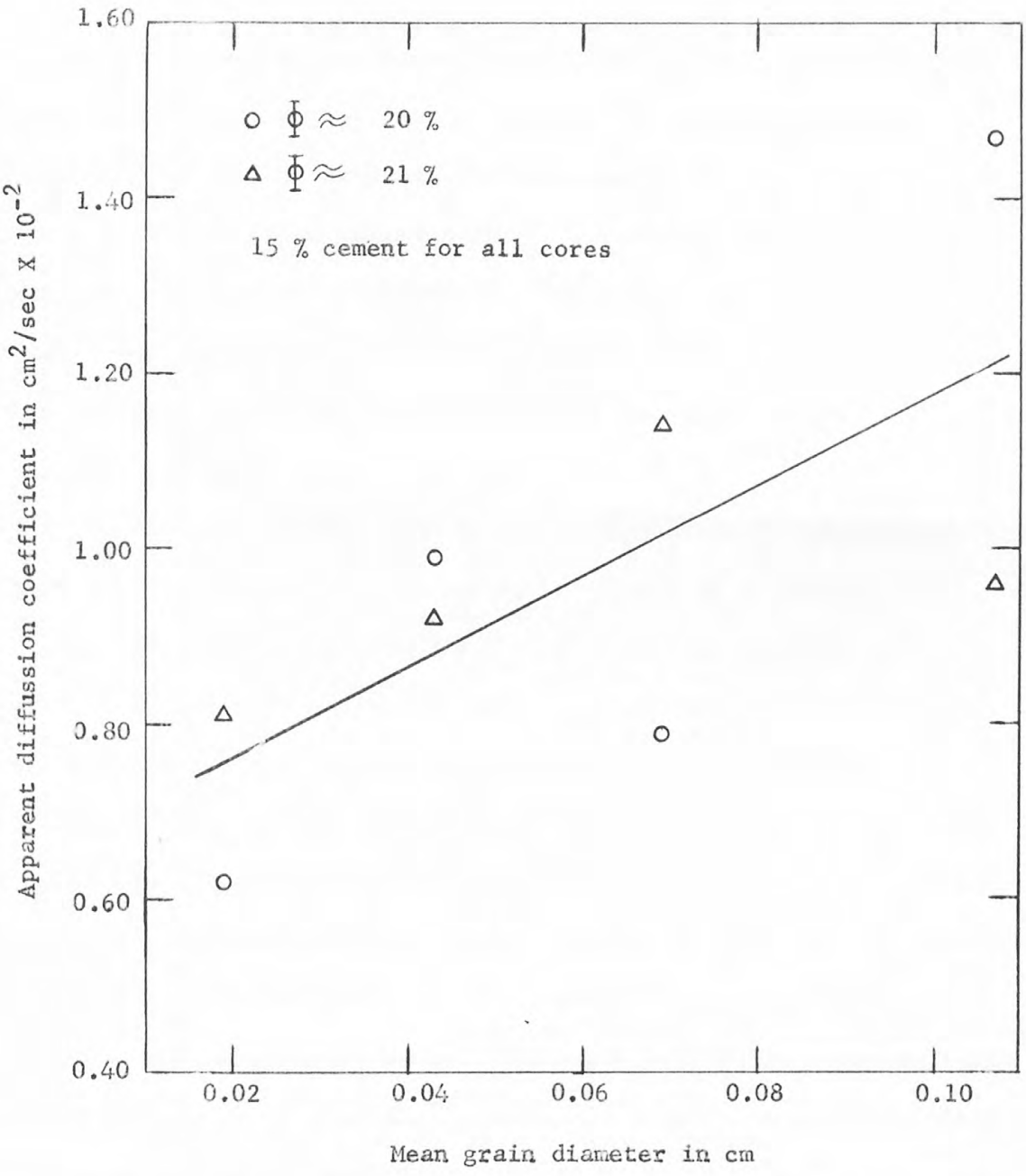

FIGURE 22.- Apparent diffusion coefficient versus mean grain diameter for artificial cores of 15 percent cement and porosities of 20 percent and 21 percent.

SUMMARY

In order to obtain porous media in which any desired combination of porosity, grain size, and cement content was readily available, three series of artificial sandstone cores were constructed by compressing a mixture of Ottawa sand grains (or plastic beads) and moist Grefco cement in a steel core barrel. The desired porosity or permeability was obtained by controlling the construction pressure. For the permeability and diffusion measurements the cores were sealed in lucite and the ends were cut off.

A plot of permeability versus porosity for cores having a range of porosities (with grain size constant) resulted in a relation between the permeability in millidarcys (k) and the fractional porosity (Φ) of the form $k = \alpha e^{\beta\Phi}$ where β is a non-dimensional factor depending on the cement content and α (cm^2) is apparently related to the grain size. A maximum value of β occurred for cores containing 20 percent cement and the factor β decreased for cores containing cement contents either greater or less than 20 percent. A plot of the permeability in millidarcys (k) versus the grain size in cm (g) for cores with cement content and porosity constant resulted in a curve of the form $k = \gamma g^{\sigma}$ where σ and γ are factors depending on the cement content and porosity.

A diffusion system was designed so that the apparent diffusion coefficient of radon diffusing through argon-saturated cores could be measured. The diffusion system consisted of two ionization chambers, one containing radon in argon and one containing argon only, connected

by a section of tygon tubing in which a core was clamped, two electrometers to measure the ionization current in the two chambers and two recorders to chart the change in radon concentration in the two chambers as a function of time. Two diffusion systems were used in measuring the apparent diffusion coefficients. In the original diffusion system a valve was used to isolate a chamber containing radon and argon from a chamber containing argon only. The diffusion of radon through a core was initiated by opening the valve. In the modified diffusion system, the valve was replaced by a small glass disc so that the separation between the chambers was reduced from about 20 cm to about 6 cm. In this system, the glass disc was shattered to initiate the diffusion of radon through the core. The radon was obtained by boiling standard radium chloride solutions containing either 10^{-9} gm or 10^{-7} gm of radium.

The apparent diffusion coefficients of three series of cores measured in the original diffusion system were corrected for the effect of the longer diffusion path in the connecting tygon tubing and valve by measuring the apparent diffusion coefficients of four cores of each series in the modified system and adjusting the apparent diffusion coefficients of the remainder of the cores in each series to values corresponding to measurements in the modified system by an amount dependent on the length of the core.

The apparent diffusion coefficients of cores having a constant grain size and porosity but different cement contents were larger for cores of lower cement content. The apparent diffusion coefficients of cores containing cement contents between 32.5 percent and 15 percent increased gradually for decreasing cement content, and the apparent

diffusion coefficient of the core containing 10 percent cement was considerably higher than that of the core containing 15 percent cement. The apparent diffusion coefficient of the core containing 40 percent cement was considerably lower than that of the core containing 32.5 percent cement.

The apparent diffusion coefficients of cores having a constant cement content and grain size but a range of porosities, increased with increasing porosity. The relation between the apparent diffusion coefficient D_a (cm^2/sec) and the porosity Φ (%) of these cores appears to be of the form $D_a = \psi \Phi^{\epsilon}$ where ψ (cm^2/sec) and ϵ (dimensionless) are factors dependent on the grain size and cement content. The present data are insufficient to assign a value to the factor ϵ.

The apparent diffusion coefficient of eight cores containing the same cement content and having approximately the same porosity (four of 20 percent porosity and four of 21 percent porosity) but representing four different grain sizes (.019cm, .043 cm, .069 cm, and 0.107 cm), appear to increase with increasing grain size. However, the apparent diffusion coefficients for any two cores representing a particular grain size were far from identical and no clear relation between a parent diffusion coefficient and grain size could be established using the available data.

In general, plots of the A/L' ratio, and the effective directional porosity did not contribute significantly to the determination of relationships between the apparent diffusion coefficient and other core characteristics.

APPENDIX I

Solutions of diffusion equation for non-stationary state of flow

For the system of figure 5, the boundary conditions are, using the substitution $c = Ce^{-\lambda t}$,

$$V_1 \frac{\partial C}{\partial t} + DA \frac{\partial C}{\partial x} = 0 \quad \text{at} \quad x = 0 \text{ for all } t,$$

$$V_2 \frac{\partial C}{\partial t} - DA \frac{\partial C}{\partial x} = 0 \quad \text{at} \quad x = L \text{ for all } t,$$

$$C = C_{10} \text{ at } x = 0,\ t = 0,\ C = 0 \text{ at } x = L,\ t = 0, \text{ and } C = 0,\ 0 < x < L,\ t = 0.$$

In this case, $x = 0$ corresponds to the end of the core near chamber A and $x = L$ corresponds to the end of the core near chamber B.

A solution of the diffusion equation $(\partial C/\partial t = D\,\partial^2 C/\partial x^2 - \lambda C)$ is of the form

$$C(x,t) = C_{10}(1 - x/L) + e^{-(a^2 D)t}(F \cos ax + G \sin ax) \qquad (14)$$

in which a, F, and G, must be evaluated. Imposing the boundary conditions on the transient part of the equation leads to the transcendental equation

$$\tan aL = \frac{Aa(V_1 + V_2)}{A^2 - a^2 V_1 V_2} \qquad (15)$$

where V_1 and V_2 are the volumes of the chambers, A is the area of the core and L is the length of the core. The coefficients F and G are partially determined by the boundary conditions so that $F/G = A/V_1 a$. Substituting $z = aL$ in (10) gives

$$\tan z = \frac{za(V_1 + V_2)}{A^2 L - z^2/L\, V_1 V_2}. \qquad (16)$$

The roots of (11) can be obtained graphically from the intersection of the curves

$$\tan \zeta = \gamma, \text{ and } \frac{\zeta A (V_1 + V_2)}{A^2 L - \zeta^2 / L \, V_1 V_2} = \gamma.$$

For each value of ζ, a corresponding value of α can be found from $\alpha = \zeta / L$ or $\alpha_n = \zeta_n / L$ (since there are infinitely many roots). A graphical solution of this type is necessary for each core unless the length and area of all cores are the same.

When the α's have been determined for a particular core, equation (14) becomes

$$C(x,t) = C_{10}(1 - x/L) + \sum_{n=1}^{\infty} e^{-(\alpha_n^2 D)t} G_n \left[\frac{A V_1}{\alpha_n} \cos \alpha_n x + \sin \alpha_n x \right] \quad (17)$$

where n is an integer. It is necessary to determine values of G_n such that $C(x,t)$ reduces to zero when $t = 0$. This requires that

$$C_{10}(1 - x/L) + \sum_{n=1}^{\infty} \left(\frac{A V_1}{\alpha_n} \cos \alpha_n x + \sin \alpha_n x \right) = 0. \quad (18)$$

The complete solution, with G_n known, is difficult to obtain although solutions under simplifying assumptions have been presented by Baranov and Gracheva (1937), Gordon (1945), and Barrer (1951).

A solution of the diffusion equation was obtained by Baranov and Gracheva (1937) for a radioactive gas source (at $x = h$) and a detecting chamber (at $x = 0$) separated by a rock layer of thickness h. The boundary conditions were: at $x = 0$, $c = 0$ and at $x = h$, $\phi = D \partial c / \partial x$.

Their solution was:

$$C=\frac{\phi}{\sqrt{D\lambda}}\left[\frac{e^{\sqrt{\lambda/D}\,x}-e^{-\sqrt{\lambda/D}\,x}}{e^{\sqrt{\lambda/D}\,h}-e^{-\sqrt{\lambda/D}\,h}}-2\pi\tan\left(\sqrt{\lambda/D}\,h\right)\sum_{1}^{\infty}\frac{(-1)^{n-1}\,n\,\sin\frac{n\pi}{h}x}{n^2\pi^2+\lambda/D\,h}\;e^{-\left[D(n^2\pi^2/h^2)+\lambda\right]t}\right] \tag{19}$$

where C is the concentration (curies/liter), ϕ is the flux of radioactive gas issuing from the source per unit time (curies/cm^2 sec), D is the diffusion coefficient (cm^2/sec), h is the layer thickness (cm), n is an integer, and λ is the decay constant of the radioactive gas.

Where the diffusion time is sufficiently short, the change in concentration of the radioactive gas in chamber A can be neglected, and the concentration in chamber A does not differ appreciably from zero. In this case, a solution of the diffusion equation is less difficult to obtain. If $x=0$ corresponds to the end of the core near chamber A and $x=L$ corresponds to the end of the core near chamber B, the boundary conditions are

$$x=0,\quad C=C_{10},\quad t=0$$

$$x=L,\quad C=0,\quad t=0.$$

Assuming the solution of $\partial C/\partial t=D(\partial^2C/\partial x^2)-\lambda C$ is of the form $C(x,t)=U(x)+V(x,t)$, separating variables in $\partial x/\partial t=D(\partial^2C/\partial x^2)-\lambda C$, and applying these boundary conditions gives

$$U(x)=C_{10}\,(1-x/L) \tag{20}$$

and

$$V(x,t)=e^{-(\lambda+a^2D)t}\left(F\cos ax+G\sin ax\right) \tag{21}$$

then

$$C(x,t) = C_{10}(1 - x/L) + e^{-(\lambda + a^2 D)t}(F \cos ax + G \sin ax) \quad (22)$$

where a is a constant, D is the diffusion coefficient, and λ is the decay constant of the radioactive gas.

Since a solution of the diffusion equation exists for $t=0$, $v(0,t)=0$ and $v(L,t)=0$. Applying these conditions to equation (21) gives $F=0$, $\sin aL=0$, and $a=n\pi/L$ (n an integer). Then

$$v(x,t) = \sum_{n=1}^{\infty} G_n \sin \frac{n\pi}{L} x \; e^{-\left(\frac{n^2\pi^2}{L^2}D + \lambda\right)t} . \quad (23)$$

The G_n's are coefficients in the half range sine expansion of the function $-C_1(1 - x/L)$ and are given by

$$G_n = \frac{2}{L}\int_0^L \left[-C_1(1 - x/L)\right] \sin \frac{n\pi x}{L} \, dx \quad (24)$$

or

$$G_n = -\frac{2C_{10}}{n\pi} \quad (25)$$

so that

$$C(x,t) = C_{10}(1 - x/L) + \sum_{n=1}^{\infty}\left(\frac{-2C_{10}}{n\pi}\right) \sin \frac{n\pi x}{L} \, e^{-\left(\frac{n^2\pi^2}{L^2}D + \lambda\right)t} . \quad (26)$$

When solutions of the diffusion equation are known, the diffusion coefficient can be evaluated from the geometry of the diffusion system and the measured concentrations in the two chambers.

APPENDIX II

Tables of artificial sandstone characteristics

Table 3a

Construction pressure and porosity for cores of 25 percent cement and medium grain size (see fig. 3)

Core	Construction pressure (psi)	Porosity (%)
R	28,400	12.0
C	26,700	12.2
4	12,400	14.5
L	10,700	15.0
H	11,600	15.0
95	5,300	16.7
52	3,600	17.2
94	3,600	18.8
123	3,400	19.9
60	2,600	20.3
8	2,200	20.6
96	2,600	21.0
109	2,300	21.2
53	2,200	22.2
110	1,600	23.7
104	2,100	23.9
2	1,300	24.2

Table 3b

Construction pressure and porosity for cores of 40 percent cement and medium grain size (see fig. 3)

Core	Construction pressure (psi)	Porosity (%)
2	7,100	10.0
2	3,600	13.0
155	1,800	15.7
117	1,200	18.2
118	1,100	20.1
73	710	23.0

Table 4

Flow rate per unit area and pressure gradient for a typical core (see fig. 4)

Porosity (%)	Cement content (%)	Grain size (cm)	Flow Rate per unit area $\left(\frac{Q}{A}\right)\left(\frac{cm}{sec}\right)$	Pressure gradient $\left(\frac{P_1 - P_2}{L}\right)\left(\frac{atm}{cm}\right)$
19.4	20	0.043	.515	.016
			.882	.027
			1.08	.034
			1.42	.044
			1.78	.055
			2.12	.067
			2.44	.077
			2.75	.036
			3.21	.102
			3.90	.123

Table 5a

Apparent diffusion coefficient of sections of a natural sandstone for the original diffusion system (see fig. 6)

Core	Porosity (%)	Length (cm)	Apparent diffusion coefficient ($cm^2/sec \times 10^{-2}$)
S	16.6	1.96	0.56
S_1	16.6	0.93	0.37
S_2	16.6	0.93	0.39
S_{21}	16.6	0.36	0.27
S_{22}	16.6	0.36	0.29

Table 5b

Apparent diffusion coefficient of sections of a natural sandstone for the modified diffusion system (see fig. 6)

Core	Porosity (%)	Length (cm)	Apparent diffusion coefficient ($cm^2/sec \times 10^{-2}$)
S_1	16.6	0.93	0.56
S_{22}	16.6	0.36	0.58

Table 6

Radon concentration in ionization chambers A and B and time after diffusion begins (see fig. 8)

Time (minutes)	Chamber A radon concentration (μμc)	Chamber B radon concentration (μμc)
0	9860	0.00
15		5.00
30	9720	15.0
60	9650	50.0
90		80.0
120	9510	120.
150		160.
180	9360	200.
210		240.
240	9210	280.

Table 7a

Permeability and porosity for cores of 15 percent cement and medium grain size (see fig. 10)

Core	Permeability (millidarcys)	Porosity (%)
46	48.8	16.0
169	50.3	16.3
43	65.2	17.5
50	79.8	18.1
100	171.	18.9
9	127.	19.0
148	161.	19.7
147	167.	20.3
131	166.	20.4
22	375.	21.0
129	379.	22.1
130	408.	22.9
84	1020.	23.3
83	1590.	24.3

Table 7b

Permeability and porosity for cores of 10 percent cement and medium grain size (see fig. 10)

Core	Permeability (millidarcys)	Porosity (%)
112	54.1	19.1
111	66.5	19.1
140	70.1	20.0
138	73.2	20.2
139	77.8	20.4

Table 7c

Permeability and porosity for cores of 15 percent cement (half Grefco, half clay) and medium grain size (see fig. 10)

Core	Permeability (millidarcys)	Porosity (%)
15	102.	19.6
26	170.	21.9
24	210.	22.3
27	340.	24.0

Table 8

Permeability and porosity for cores of 20 percent cement and medium grain size (see fig. 11)

Core	Permeability (millidarcys)	Porosity (%)
115	13.0	13.5
116	13.2	14.2
114	23.1	14.5
162	43.9	15.5
160	70.3	16.5
146	54.1	17.5
144	85.1	18.0
145	90.0	18.3
92	172.	19.4
72	306.	20.1
70	552.	20.2
165	187.	20.4
71	619.	20.7
127	709.	21.4
126	1080.	21.9
164	448.	21.5
149	776.	21.8
128	1040.	22.0
149	1410.	22.0
101	1250.	22.2
150	1380.	22.2
102	1710.	23.6

Table 9a

Permeability and porosity for cores of 32.5 percent cement and medium grain size (see fig. 12)

Core	Permeability (millidarcys)	Porosity (%)
64	10.4	14.8
105	14.3	15.4
66	14.2	15.2
134	24.2	16.1
106	30.6	16.4
56	35.9	17.3
55	63.0	19.8
62	68.1	20.1
63	77.4	20.1
122	53.9	20.5
68	124.	21.4
91	102.	21.8
69	176.	24.7
120	328.	24.7
67	242.	26.7
121	827.	32.7

Table 9b

Permeability and porosity for cores of 25 percent cement and medium grain size (see fig. 12)

Core	Permeability (millidarcys)	Porosity (%)
R	10.2	12.0
C	10.0	12.2
4	40.6	14.7
H	42.1	15.0
L	33.0	15.0
95	86.0	16.7
52	121.	17.2
94	159.	18.8
123	221.	19.9
60	251.	20.3
8	246.	20.6
96	306.	21.0
109	344.	21.2
53	417.	22.2
110	838.	23.7
104	878.	23.9

Table 10

Permeability and porosity for cores of 40 percent cement and medium grain size (see fig. 13)

Core	Permeability (millidarcys)	Porosity (%)
G	9.00	13.2
7	11.0	15.4
155	10.1	15.6
156	9.27	16.4
132	15.8	17.6
133	21.5	18.6
75	37.5	19.8
118	22.4	20.1
119	30.4	20.9
173	62.1	22.4
107	52.5	22.5
172	96.9	25.1
108	216.	28.3
74	226.	29.2

Table 11

Permeability and cement content for cores of 20 percent porosity and medium grain size (see fig. 14)

Core	Cement content (%)	Permeability (millidarcys)
140	10.0	73.2
147	15.0	167.
72	20.0	306.
60	25.0	251.
62	32.5	68.1
118	40.0	22.4

Table 12

Construction pressure and cement content for cores of 20 percent porosity and medium grain size (see fig. 15)

Core	Construction pressure (psi)	Cement content (%)
140	41,000	10.0
147	9,100	15.0
72	6,200	20.0
60	2,600	25.0
62	1,400	32.5
118	1,100	40.0

Table 13

Permeability and grain size for cores of 20 percent porosity and 15 percent cement (see fig. 16)

Core	Permeability (millidarcys)	Grain size (cm)
158	42,3	.019
147	166.	.043
36	539.	.069
38	1490.	.107

Table 14

Correction data for apparent diffusion coefficients of original and modified diffusion systems(see figs. 17a, 17b, 17c)

Core	Cement content (%)	Core length (cm)	Apparent diffusion coefficient ($cm^2/sec \times 10^{-2}$) (original diffusion system)	Apparent diffusion coefficient ($cm^2/sec \times 10^{-2}$) (modified diffusion system)
(a)				
147	15	1.95	0.78	0.99
72	20	1.53	0.73	0.95
60	25	1.75	0.73	0.93
118	40	1.31	0.40	0.48
(b)				
140	10	2.09	0.93	1.17
147	15	1.95	0.78	0.99
72	20	1.53	0.73	0.95
60	25	1.75	0.73	0.93
62	32.5	2.06	0.68	0.91
118	40	1.31	0.40	0.48

Table 15

Apparent diffusion coefficients in original and modified diffusion systems and cement contents for cores of 20 percent porosity and medium grain size (see fig. 18)

Core	Cement content (%)	Apparent diffusion coefficient ($cm^2/sec \times 10^{-2}$) (original diffusion system)	Apparent diffusion coefficient ($cm^2/sec \times 10^{-2}$) (modified diffusion system)
140	10	0.93	1.17
147	15	0.78	0.99
72	20	0.73	0.95
60	25	0.73	0.93
62	32.5	0.68	0.91
118	40	0.40	0.40

Table 16

Lithologic factor and cement content for cores of 20 percent porosity and medium grain size (see fig. 19)

Core	Cement content (%)	Lithologic factor, (dimensionless)
140	10	1.99
147	15	2.36
72	20	2.43
60	25	2.51
62	32.5	2.54
118	40	4.82

Table 17

Apparent diffusion coefficient and porosity for cores of 15 percent cement and medium grain size (see fig. 20)

Core	Porosity (%)	Apparent diffusion coefficient ($cm^2/sec \times 10^{-2}$)
46	16.0	0.72
43	17.5	0.77
9	19.0	0.87
148	19.7	0.68
147	20.3	0.99
131	20.4	0.95
22	21.0	1.05
129	22.1	1.19
84	23.3	1.00
83	24.3	1.02

Table 18

Effective area and porosity for cores of 15 percent cement and medium grain size (see fig. 21)

Core	Porosity (%)	Effective area, A' (cm^2)
46	16.0	0.178
43	17.5	0.170
9	19.0	0.212
148	19.7	0.140
147	20.3	0.209
131	20.4	0.201
22	21.0	0.253
129	22.1	0.235
84	23.3	0.197
83	24.3	0.194

Table 19

Apparent diffusion coefficient and mean grain diameter for cores of 20 percent and 21 percent porosity and 15 percent cement (see fig. 22)

Core	Apparent diffusion coefficient ($cm^2/sec \times 10^{-2}$) (20 percent porosity)	Mean grain diameter (cm)	Core	Apparent diffusion coefficient ($cm^2/sec \times 10^{-2}$) (20 percent porosity)
13	0.81	0.019	158	0.62
131	0.92	0.043	147	0.99
37	1.14	0.069	36	0.79
40	0.96	0.107	38	0.71

APPENDIX III

Table of symbols

Symbol	Units	Description
k	millidarcys	Permeability
Φ	percent or fractional	Porosity
g	cm	Mean grain diameter
D_o	cm^2/sec	True diffusion coefficient
D_a	cm^2/sec	Apparent diffusion coefficient
∇		Laplacian operator
c	curies/liter or equivalents/liter	Concentration (general equation)
λ	sec^{-1}	Decay constant
ϕ, ε, Q	curies/cm^2 sec	Flux
L	cm	Length of core
A	cm^2	Area of core
h	cm	Thickness of layer
I	curies/cm^2 sec	Flux through layer of particular thickness
A'	cm^2	Effective core area
L'	cm	Effective core length
V	cm^3	Volume of chamber
t	sec	Time
ΔC_o	curies/liter or equivalents/liter	Initial concentration difference between two chambers or compartments
ΔC_t	curies/liter or equivalents/liter	Concentration difference between two chambers or compartments at time t
η	gm/cm sec	Viscosity

Symbol	Units	Description
$\bar{Q}$	cm^3/sec	Flow rate at average pressure across core
P_1 & P_2	atmospheres	Pressure at end of core
$\mu\mu C$	disintegrations/sec x 10^{-12}	Activity or concentration
b	cm^{-2}	Cell factor
Δt	sec	Time interval
q	$\mu\mu C$/sec	Quantity of radon entering chamber in interval
p	$\mu\mu C$/sec	Recorded quantity of radon entering chamber in time interval
$F(t+\frac{\Delta t}{2})$	fractional	Average equilibrium fraction
H_i	sec	$\sum_{i=0}^{t} F\left(t_1 + \frac{\Delta t}{2}\right)$
f	dimensionless	Equilibrium correction
C_0 & C_{10}	curies/liter or equivalents/liter	Initial concentration
C_t	curies/liter or equivalents/liter	Concentration at time t
α	cm^2	Proportionality factor
β	dimensionless	Exponent
γ		Proportionality factor
σ	dimensionless	Exponent
ψ	cm^2/sec	Proportionality factor
ϵ	dimensionless	Exponent
F & G	dimensionless	Proportionality factors
a	dimensionless	Constant
^oC	degree centigrade	Temperature
D	cm^2/sec	Diffusion coefficient (general equations)

SELECTED REFERENCES

Alvarez, Manuel, 1949, Porosity and permeability in relation to gas injection in an oil field: Petroleos Mexicanos, no. 72, p. 100-111.

Alverti, G., and Lovera, G., 1949, The efflux of radon from the soil: Annali Geofisica (Rome) 2, v. 43, no. 1, p. 137-141.

Bagnall, K. W., 1957, Chemistry of the Rare Radio-elements, New York, Adademic Press, Inc., 177 p.

Baranov, V. I., and Gracheva, E. H., 1937, Method of studying the permeability of rocks to radioactive emanations: State Radium Inst. (USSR) Trans., v. 3, p. 117-122. (In Russian).

Baranov, V. I., and Novitskaya, A. P., 1949, Diffusion of radon in native muds: Trudy Biogeokhim. Lab., Akad. Nauk. SSSR, no. 9, p. 163-171. (In Russian).

Barrer, R. M., 1951, Diffusion in and through solids: Cambridge, The University Press, 464 p.

Blake, G. R., and Page, J. B., 1948, Direct measurement of gaseous diffusion in soils: Soil Sci. Soc. America. Proc., v. 13, p. 37-43.

Brownell, L. E., and Katz, D. L., 1947, Flow of fluids through porous media. I. Single homogenous fluids: Chem. Eng. Prog., v. 43, p. 537.

Buckingham, E., 1904, Contributions to our knowledge of the aeration of soils: U. S. Dept. Agr., Bur. Soils, Bull. no. 25.

Budde, E., 1958, Radon measurements as a geophysical method: Geophys. Prosp. v. 6, no. 1, p. 25-34.

Bulashevich, Y. P., 1947, Diffusion of radon in the soil taking convection into consideration: Acad. Sci., USSR, Geophys. and Geochem. ser. Bull., v. 11, no. 1 (In Russian).

Bumstead, H. A., and Wheeler, L. P., 1904, On the properties of a new radioactive gas found in the soil and water near New Haven: Am. Jour. of Sci., v. 17, no. 98, p. 97-111.

Carman, P. C., 1956, Flow of gases through porous media: New York, Academic Press, 182 p.

Carslaw, H. S., and Jaeger, J. C., 1947, Conduction of heat in solids: Oxford Clarendon Press, 386 p.

Chaumont, L., 1910, Note on the coefficient of diffusion of the radium emanation into air: Radium, v. 6, no. 4, p. 106.

Corey, A. T., and Rathjens, C. H., 1956, Effect of stratification on relative permeability: Jour. Petroleum Technology, V. 8, p. 69-71.

Crank, J., 1956, The mathematics of diffusion: Oxford, Clarendon Press, 347 p.

Cuthbertson, C., 1911, New determinations of some constants of the inert gases: Philos. Mag., v. 21, no. 6, p. 69-77.

Dallavalle, J. M., 1948, Micromeritics 2nd Edit., New York, Pitman Publishing Corporation. 555 p.

Eckmann, G., 1913, The diffusion and migration of radium A atoms: Jahrb. Radioakt. Elektronik, v. 9, p. 157-187.

Evans, D. D., 1953, Effect of combined pressure and concentration gradients on gaseous flow through soils: Iowa State Coll., Jour. Sci., v. 27, p. 165-166.

Evans, R. D., 1955, The Atomic Nucleus, New York, McGraw-Hill Book Company, Inc., 972 p.

Fancher, G. H., and Lewis, J. A., 1933, Flow of simple fluids through porous materials: Indus. Eng. Chem., v. 25, p. 1139-1147.

Fettke, C. R., 1951, Physical characteristics of Bradford Sand, Bradford Field, Penn., and relation to the production of oil: Am. Assoc. Petroleum Geologists Bull., v. 18, no. 1, p. 191.

Flegg, P. B., 1953, The effect of aggregation on diffusion of gases and vapors through soils: Jour. Sci., Food Agr., v. 4, p. 104-108 .

Flugge, S., and Zimens, K. E., 1939, Determination of grain size and diffusion constant from the emanating power. Theory of emanation methods: Zhur. Physik. Chem., B 42, p. 179-220.

Furnas, C. C., 1928, The flow of gases through beds of broken solids: U. S. Bur. Mines Bull. 307, 21 p.

Furry, W. H., 1948, The elementary explanation of diffusion phenomena in gases: Am. Jour. Physics, v. 16, p. 63-78.

Garrels, R. M., Dryer, R. M., and Howland, A. L., 1949, Diffusion of ions through intergranular spaces in water-saturated rocks: Geol. Soc. America Bull., v. 60, p. 1809-1828.

Gemant, A. J., 1953, Tracer diffusion in the ground in radioactive leak location: Appl. Physics, v. 24, p. 93-95.

Gentner, W., and Trendelenburg, E. A., 1954, A mass spectrometric method for the determination of the diffusion constants of gases in solid bodies: Zhur. Naturforsch., v. 9a, p. 802-804.

Gordon, A. R., 1945-1946, The diaphragm cell method of measuring diffusion: N. Y. Acad. Sci., Ann., v. 46, p. 285-308.

Gracheva, E. G., 1938, The effect of structure and porosity of rocks on the diffusion of radioactive emanations: State Radium Inst. (USSR) Trans., v. 4, p. 228-233 (English Summary).

Grammakov, A. G., 1936, The influence of some factors on the spreading of radioactive emanations in natural conditions: Zhur. Geofisiki, v. 6, p. 123-148.

Grammakov, A. G., and Lyathkovskaya, N. M., 1935, On Diffusion of radioactive emanations in rocks: Zhur. Geofisiki, v. 6, p. 123-148 (In Russian).

Harrington, E. L., 1920, Experimental evidence of the existence of aggregates of active deposit atoms in gases containing radon: Philos. Mag., v. 6, no. 37, p. 685-695.

Harrison, G. E., 1942, The thermal diffusion of radon gas mixtures: Royal Soc. Proc (London), v. A181, p. 93-100.

Harned, H. S., and French, D. M., 1945-1946, A conductance method for the determination of the diffusion coefficients of electrolytes: N. Y. Acad. Sci., Ann., v. 46, p. 267-284.

Hirst, W., and Harrison, E. G., 1938-1939, The diffusion of radon gas mixtures: Royal Soc. Proc., Ser. A, v. 169, p. 573-586.

Israel-Kohler, H., and Becker, F., 1936, Emanation relations in ground air: Gerlands Beitr. Geophys., v. 48, p. 13-58.

Jost, Wilhelm, 1952, Diffusion in solids, liquids, gases: New York, Academic Press, 558 p.

Klinkenberg, L. J., 1951, Analogy between diffusion and electrical conductivity in porous rocks: Geol. Soc. America Bull., v. 62, p. 559-564.

Kryukov, S. N., and Zhukhovitskie, A. A., 1953, A method for determining diffusion coefficients: Doklady Akad. Nauk. SSSR, v. 90, p. 379-382 (In Russian).

Leslie, M. S., 1912, A comparison of the coefficients of diffusion of thorium and actinum emanations, with a note on their periods of transformation: Philos. Mag., v. 24, p. 637-647.

Levorsen, A. I., 1956, Geology of Petroleum, San Francisco, W. H. Freeman and Company, 703 p.

Mandel, Peter, Jr., Berg., J. W., Jr., and Cook, K. L., 1957, Resistivity studies of metalliferous synthetic cores: Geophysics, v. 22, no. 2, p. 398-411.

Martin, J. J., and McCabe, W. L., and Monrad, C. C., 1951, Pressure drop through stacked spheres: Chem. Eng. Prog., v. 47, p. 91-95.

McLennan, J. C., 1912, On the diffusion of actinium emanation and the active deposit produced by it: Philos. Mag., v. 24, no. 141, p. 370-379.

Mortari, N., 1933, A simple method for determining the diffusion coefficient of radium emanation: Atti. Accad. Lincei, v. 17, p. 949-951.

Murphy, W. O., Jr., Berg, J. W., Jr., and Cook, K. L., 1957, Seismic velocity study of synthetic cores: Geophysics, v. 22, no. 4, p. 813-820.

Muskat, Morris, 1937. The flow of homogeneous fluids through porous media: New York, McGraw-Hill Book Co., Inc., 763 p.

Muskat, Morris, and Botset, H. G., 1931, Flow of gas through porous materials: Physics v. 1, p. 27-47.

Nevin, C. M., 1932, Permeability its measurement and value: Amer. Assoc. Petroleum Geologists Bull., v. 16, no. 4, p. 364-373

Paine, L. M., 1956, Petrophysical analysis of some Wilcox wells: Jour. Petroleum Technology, v. 8, p. 25-31.

Penman, H. G., 1940, Gas and vapor movements in the soil: Jour. Agr. Sci., v. 30, p. 437-462 and p. 570-581.

Prager, Stephen, 1951, The calculation of diffusion coefficients from sorption data: Jour. Chem. Physics, v. 19, no. 5, p. 537-541.

Rankine, A. O., 1911, Relation between viscosity and atomic weight for the inert gases, with its application to the case of radium emanations: Philos. Mag., v. 21, no. 6, p. 45-53.

Rogers, A. S., 1958, The physical behavior and geologic control of radon in mountain streams: U. S. Geol. Survey Bull. 1052-E, p. 187-211.

Rogers, W. A., Buritz, R. S., and Alpert, D. A., 1954, Diffusion coefficient, solubility, and permeability for helium in glass: Jour. Appl. Physics, v. 25, no. 7, p. 868-875.

Róna, Elizabeth, 1917, rate of diffusion and diameter of the atom of radium emanations: Zhur. Physik Chem., v. 92, p. 213-219.

Russ, Sidney, 1909, The diffusion of actinium and thorium emanations: Philos Mag., no. 6, v. 17, p. 412-422.

Satterly, John, 1911, A study of the radium emanation contained in the air of various soils: Camb. Philos. Soc. Proc., v. 16, p. 336-355.

Scheidegger, A. E., 1957, The physics of flow through porous media: New York, The Macmillan Co., 236 p.

Schwertz, F. A., and Brow, J. E., 1951, Diffusivity of water vapor in some common gases: Jour. Chem. Physics, v. 19, no. 5, p. 640-646.

Sheinker, N. S., 1948, Generalized equation of diffusion through porous membranes and its practical utilization: Kolloid Zhur., v. 10, p. 382-393.

Taylor, G. S., and Abrahams, J. H., 1953, Diffusion-equilibrium method for obtaining gases under field conditions: Soil Sci. Soc. America Proc. 17, p. 201-206.

Von Haul, R. A. W., 1954, Separation of isotopes by means of surface diffusion in porous media: Naturewissenschaften 41, p. 255-256.

Wellisch, E. M., 1910, Laws of mobility and diffusion of the ions formed in gaseous media: Camb. Philos. Soc. Proc., v. 15, p. 1-10.

Wyckoff, R. D., Botset, H. G., Muskat, Morris, and Reed, D. W., 1934, Measurement of permeability of porous media: Am. Assoc. Petroleum Geologists Bull., v. 18, no. 2, p. 161-190.

Ziemens, K., 1943, Surface determinations and diffusion measurements by means of radioactive inert gases. III. The process of emission of the radiation from disperse systems: Zhur. Physik. Chem., v. 192, p. 1-55.

Zimens, K. E., 1942, Surface determinations and diffusion measurements by radioactive noble gases. Practice and quantitative method. I. The practical procedure of measuring. II. The valuation of data: Zhur. Physik. Chem., A191, p. 1-53.


BOUND BY
HNM